INFORMATION TO USERS

This manuscript has been reproduced from the microfilm master. UMI films the text directly from the original or copy submitted. Thus, some thesis and dissertation copies are in typewriter face, while others may be from any type of computer printer.

The quality of this reproduction is dependent upon the quality of the copy submitted. Broken or indistinct print, colored or poor quality illustrations and photographs, print bleedthrough, substandard margins, and improper alignment can adversely affect reproduction.

In the unlikely event that the author did not send UMI a complete manuscript and there are missing pages, these will be noted. Also, if unauthorized copyright material had to be removed, a note will indicate the deletion.

Oversize materials (e.g., maps, drawings, charts) are reproduced by sectioning the original, beginning at the upper left-hand corner and continuing from left to right in equal sections with small overlaps. Each original is also photographed in one exposure and is included in reduced form at the back of the book.

Photographs included in the original manuscript have been reproduced xerographically in this copy. Higher quality 6" x 9" black and white photographic prints are available for any photographs or illustrations appearing in this copy for an additional charge. Contact UMI directly to order.

UMI®

Bell & Howell Information and Learning
300 North Zeeb Road, Ann Arbor, MI 48106-1346 USA
800-521-0600

The Influence Of Second-Order Motion On The Induction Of Vection

Cindy J. Potechin

A Thesis

in

The Department

of

Psychology

Presented in Partial Fulfillment of the Requirements
for the Degree of Master of Arts at
Concordia University
Montreal, Quebec, Canada

August 1998

ABSTRACT

The Influence Of Second-Order Motion On The Induction Of Vection

Cindy Potechin

Optical flow fields composed of spatiotemporal luminance modulations (first-order) versus spatiotemporal contrast modulations (second-order) differ in their ability to induce the illusions of motion aftereffect (MAE) and structure from motion. The inability of second-order (SO) motions to support structure from motion except in response to simple motion stimuli has led to the suggestion that SO motions cannot support computations relating to motion-in-depth. Three experiments were used to determine the ability of first-order (FO) and SO motion stimuli to induce vection, the illusion of 3-D motion induced by image flow. Subjects reported the duration and latency to onset of the MAE and vection illusions in response to stimuli composed of mulitiplicative combinations of a basic vection signal (radially expanding concentric rings) with three different carriers. The stimulus patterns contained different amounts of FO and SO motion energy (ME). The results indicated that a SO motion signal can induce vection but the vection responses will have slower onsets and shorter durations than those induced by a FO motion signal. As well, the vection response to the SO signal is not the result of contamination by FO artifacts, suggesting that the visual system contains a mechanism specialized for the detection of SO motions and that the activation of these mechanisms is sufficient to induce a sense of self-motion.

Acknowledgements

Sometimes one's life can also be affected in profound ways by events which seem insignificant at the time. In my case, it was an offhand remark by a man I did not know. When I heard this man describe the difference between a person who holds a graduate degree and one who does not as a vast amount of hard work, I was determined to be the holder of a graduate degree. However, I could not have brought this project to completion without the abilities I developed under my father's consistent influence and wisdom during the time we shared. By his example, I discovered that one should never stop learning and growing. His legacy to me was the love of knowledge and the drive to carry through a project to the best of my ability, two things that will help me to continue on with my work now that my father is gone.

I would like to express my heartfelt thanks to Rick Gurnsey, under whose supervision this research was conducted. Dr. von Grünau and Dr. Bross, thank you for the helpful comments you gave me which allowed me to make this work more complete and easier for the average person to read.

Of course, I would not be able to get away without acknowledging the constant support of my best friend Richard (He told me to put this in!).

Last but not least, I am especially grateful to my subjects, a hardy lot, who came in for repeated torture (er...test) sessions but who rarely complained and gave freely of themselves to provide the data upon which this thesis is based.

This study was supported in part by an FCAR grant to the author.

Table of Contents

List of Figures

List of Tables

The Influence Of Second-Order Motion On The Induction Of Vection

Motion processing is so crucial to our survival that Nakayama (1985) described it as a fundamental biological sense, as basic as sensitivity to contrast and color. Visual motion processing subserves many functions including the co-ordination of head and body movements, the avoidance of collision with objects in the environment, and the separation of objects from their backgrounds. Researchers have been able to provide evidence for low-level motion detection mechanisms based on the principle of spatiotemporal energy detection to explain the detection of simple motions such as a white bar moving across a dark background. However, there are some classes of motion cannot be explained on the basis of these low-level mechanisms such as theta motion (Zanker, 1993), where an object defined by dot motion in one direction is actually moving in the opposite direction, and nonFourier motion (Chubb and Sperling, 1988), which refers to stimuli which are perceived to be moving coherently but that show no coherent direction of motion in local patches of the image. Different theories suggest that motion detection of these complex motions is either constructed late in the visual system or represents an elementary cognitive process.

The idea that motion is mediated by multiple mechanisms is a relatively recent development in motion research. Many early motion studies examined stroboscopic motion, a form of apparent motion rather than real or continuous motion. Stroboscopic motion refers to the experience of movement induced by successive presentations of stationary stimuli while real motion pertains to the continuous movement of objects. Initially, there was some concern over using apparent motion as an approximation of actual motion. Braddick (1974) suggested that apparent motion created with small displacements was processed by the same early stage mechanism which mediated the perception of continuous motion. Evidence supporting the idea that apparent motion is processed by the same mechanism as real motion was not demonstrated until 1984.

Gregory and Harris (1984) were able to present real and apparent motion in opposing directions on a single disc by using two different light sources, continuous and strobe lighting, to illuminate a rotating disc with equally spaced black and white sectors. They were able to reduce the two motions to ambiguous jitter by adjusting the relative luminances of the two light sources. The finding that real and apparent motions presented in opposing directions can cancel each other out suggested that the two motion signals are extracted by the same neural mechanism (Gregory, 1985; Gregory and Harris, 1984).

A) Short-Range versus Long-Range Motion

Braddick (1974) was the first to propose the involvement of two separate visual pathways in motion detection. In a study comparing different types of apparent motion, he found large differences in the properties of motion induced by random dot kinematograms (RDKs) and motion induced by larger displacements of large discrete forms. RDKs are pairs of images containing randomly distributed black and white dots that are alternated in time. A central region of dots is displaced uniformly from one frame to the next whereas all dots outside this region vary randomly. When the two patterns are alternated at an appropriate rate, an oscillating "object" appears to move over a background. Braddick (1974) named the two processes as long-range and short-range mechanisms because of the existence of two different maximal displacement limits (D_{max}) in the detection of apparent motion in each of the proposed motion mechanisms. Braddick pointed out a number of specific differences in the characteristics of the short-range and long-range systems including spatial range, temporal range, and the ability to detect motion dichoptically. Cavanagh and Mather pointed out the additional belief that the two systems showed differences in the ability to produce motion aftereffects (MAEs), a phenomenon where extended viewing of a unidirectional moving pattern results in an illusion of motion if the pattern subsequently stops drifting. Short-range motion was detected over short displacements and brief durations when the stimulus was observed binocularly but not

when viewed dichoptically. Additionally, short-range motion could produce MAEs. Long-range motion was detected over longer distances and longer durations and could be observed without dichoptic presentation but it could not produce MAEs.

Unfortunately, the short-range versus long-range distinction proved to be inconsistent with psychophysical evidence as was demonstrated by the following cases: 1) The so called short-range motion can be seen over large distances. Chang and Julesz (1983) showed that D_{max} is related to the size of the elements in the RDK; D_{max} can be increased by increasing the size of the RDK elements. Conversely, long range motion can be detected with small shifts in the image. Many stimuli can produce compelling impressions of motion with small displacements and it appears that the smallest displacements under which motion is detected falls into the same range as for acuity measures (Baker & Braddick, 1985). 2) Although Braddick (1974) reported a progressive deterioration in the perception of an oscillating square as the interstimulus interval (ISI) separating successive frames went from 10 to 80 msec, Mather (1988) found that apparent motion could be detected for ISIs of up to 500 msec. 3) Cavanaugh and Mather (1989) suggested that Braddick (1974) failed to show motion perception in response to dichoptically presented RDKs because after-images interfered with the motion displays. However, Cavanaugh and Mather (1989) presented a short-range motion stimulus sequence in response to which motion could be detected easily. 4) Von Grünau (1986) demonstrated that a MAE could be produced in response to long-range stimuli under the appropriate testing conditions. 5) It was assumed that short-range motion detection occurred early in the visual process and that the long-range process operated at a higher level in the visual system to detect motion through the feature tracking. Chubb and Sperling (1988) built a model to explain the responses of the visual system to both long-range and short-range stimuli using a low-level mechanism.

B) First- order (FO) versus Second-Order (SO) motion

Cavanagh and Mather (1989) suggested an alternative motion encoding dichotomy to Braddick's (1974). Their argument was that Braddick's (1974) long-range versus short-range distinction was actually a stimulus distinction which did not necessarily represent the existence of two fundamentally different mechanisms. The short-range process was based on the properties of RDKs, spatiotemporal variations in image intensity, while the traditional stimulus for long-range motion studies were individual shapes presented in succession at different spatial locations. Therefore, Cavanagh and Mather (1989) proposed two stimulus distinctions, FO and SO motion, which do not necessarily support the existence of different motion mechanisms.

FO properties are defined in terms of the dimensions of regions that vary in the image. FO stimuli are characterized by individual points that differ in terms of FO properties, luminance and possibly color. This represents information received at the earliest level of the visual system and which is conveyed through the visual system up to the level of the striate cortex with little modification. SO properties describe the frequency with which specific combinations occur for pairs of points in the image. SO images refer to image regions which have identical mean luminance but which differ in SO properties such as contrast modulation, texture, temporal modulation, or ocular distributions (depth, relative motion) of luminance. FO and SO motions refer to spatiotemporal displacements of FO and SO properties, respectively. Cavanagh and Mather (1989) suggested that separate mechanisms are required to process FO and SO motion although they did entertain the possibility that a single mechanism might be able to handle the processing of the two stimulus classes.

C) Fourier versus nonFourier motion

Chubb and Sperling (1988) proposed a distinction between Fourier and non-Fourier motion which is similar to the FO/SO distinction of Cavanagh and Mather (1989).

Stimulus movement can be represented mathematically as a spatio-temporal luminance function (such as L(x,y,t)) but it can also be expressed in terms of a spatio-temporal frequency domain by the application of a Fourier transform to the luminance function (Nakayama, 1985). Fourier stimuli refer to image motions that produce a concentration of Fourier components on a plane through the origin of the spatio-temporal frequency domain. Consequently, such motion can be extracted by Fourier based motion detectors. NonFourier stimuli are patterns that do not display a coherent shift in their intensity profile across space and time. The Fourier analyses of nonFourier stimuli do not contain a concentration of energy on a single plane in the Fourier domain and, therefore, these motions are invisible to Fourier based detectors (Chubb and Sperling, 1988). According to Mather and West (1993) SO motion stimuli correspond to a sub-set of non-Fourier motion stimuli, those involving SO contours.

Motion Detection Schemes

Theories of motion detection fall within two basic categories, feature matching and motion energy extraction. Theorists normally promote one motion detection scheme over the other but Smith (1994) argued that both computational strategies are used by the human visual system. Feature matching models were originally designed to account for the properties of apparent motion rather than continuous motion. A typical feature matching model suggests that the visual system first identifies salient image features and then tracks the position of these features over time. For example, in the minimal mapping theory of motion (Ullman, 1979), motion was detected on the basis of correspondences established between low-level image features such as points, edge fragments, and blobs. Matching models allow for the determination of velocity of features in the image (Adelson & Bergen, 1985).

Depending on how a feature is defined, feature matching models can provide a good account of the motion of FO stimuli such as a horizontally moving bar but are less

able to account for the perceived motion of SO stimuli such as beat stimuli, patterns which alternate in contrast, and contrast modulated dynamic noise. FO stimuli appear to be detected more easily than SO stimuli on the basis of feature detection but this does not imply that feature matching models cannot be used to detect SO motion. Within the feature matching framework questions such as *What constitutes a feature?* and *What exactly is being matched?* have not been satisfactorily answered. The following circumstances pose problems for the matching model: 1) The projected properties of a moving object change over time. For example, when an object is rotated, markings on the surface of an object have visually different representations over time; e.g., circles painted on a rotating cylinder will appear as ellipses at different times during the rotation, 2) different directions of local motion are perceived at different locations in the image for complex images such as random noise patterns, and 3) motion sequences can be constructed in which the objects represented in alternating frames are different but motion is perceived nevertheless. The visual system clearly perceives motion under all these conditions (Adelson & Bergen, 1985). Therefore an alternative to the feature matching model may be required to explain these phenomena.

RDKs are defined only by the displacement of a dot region over successive frames. That is, RDKs cannot be detected in a single frame alone. Therefore, it is unlikely that motion detection in RDKs is based on feature matching because motion detection precedes object identification (Zanker, 1994a). The visual system must perform a correlation type operation to encode motion of RDKs which has lead a number of theorists to promote motion energy (ME) mechanisms as an alternative to the feature matching framework (Adelson & Bergen, 1985; Wilson, Ferrera & Yo, 1992). ME models assume that the image first undergoes an initial stage of processing by linear spatiotemporal filters, followed by a squaring nonlinearity, and finally, local responses are pooled to provide an estimation of the motion phenomenon (Wilson et al., 1992).

Reichardt Type Motion Detectors

A simple type of comparator, the Reichardt type detector, has often been implicated in the ME process. In its simplest form, the Reichardt detector (Reichardt, 1961) is a direction selective system which uses a time delay to compare signals from spatially separated photoreceptors. Figure 1 represents a Reichardt detector subunit specialized for the detection of rightward motion. As the stimulus travels across the visual field, the motion signal from receptor R_1 at time t_1 is correlated with the activity of receptor R_2 at time $t_1 + \Delta t$. The signal from receptor R_1 is delayed relative to that of R_2 before the two inputs are multiplied together to form an integrated motion signal. The product of the multiplier is large when the two signals arrive at the multiplication unit at the same time, signaling a high probability of rightward motion. The Reichardt detector can process stimuli travelling within a particular range of speeds. For stimuli travelling outside of that range, the inputs of the two receptors will not reach the multiplier with sufficient overlap in time.

The Reichardt detector is composed of 2 subunits tuned to motion in opposite directions (Figure 2). To calculate the response of the detector, the response of the M_1 subunit is subtracted from the response of the M_2 subunit. That is, a positive output represents rightward motion and a negative output represents leftward motion. Each subunit can detect motion by itself but when the two subunits are combined the motion detector is better able to distinguish between non-motion stimuli, such as flicker, from continuous motion stimuli (Dosher, Landy, and Sperling, 1989).

The classic Reichardt detector was developed to explain motion detection in insects. To predict human psychophysical behavior, van Santen and Sperling (1985) developed the Elaborated Reichardt detector (ERD; Figure 3), an enhanced version of the classic motion detector. Each subunit receives inputs from two spatiotemporal filters and the output is put through a low-pass linear time filter rather than being compared using a pure time delay. The outputs of the time filter are multiplied with the other unfiltered signal and then put through a time averaging operation, to correlate the undelayed and delayed signals. Lastly,

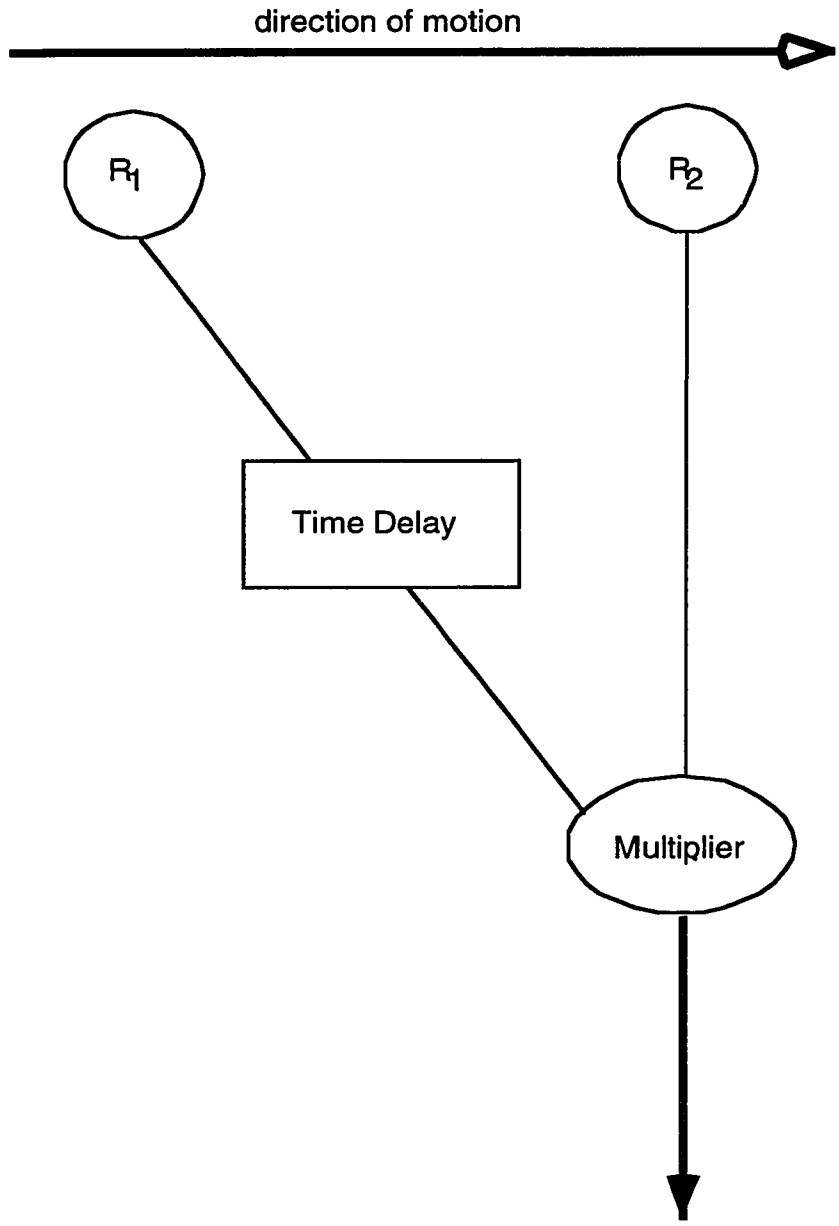

Figure 1. Schematic of the basic Reichardt detector subunit specialized for rightward motion. Visual inputs from the two retinal receptors, R1 and R2, are correlated after a time delay is applied to the signal from the leftward receptor.

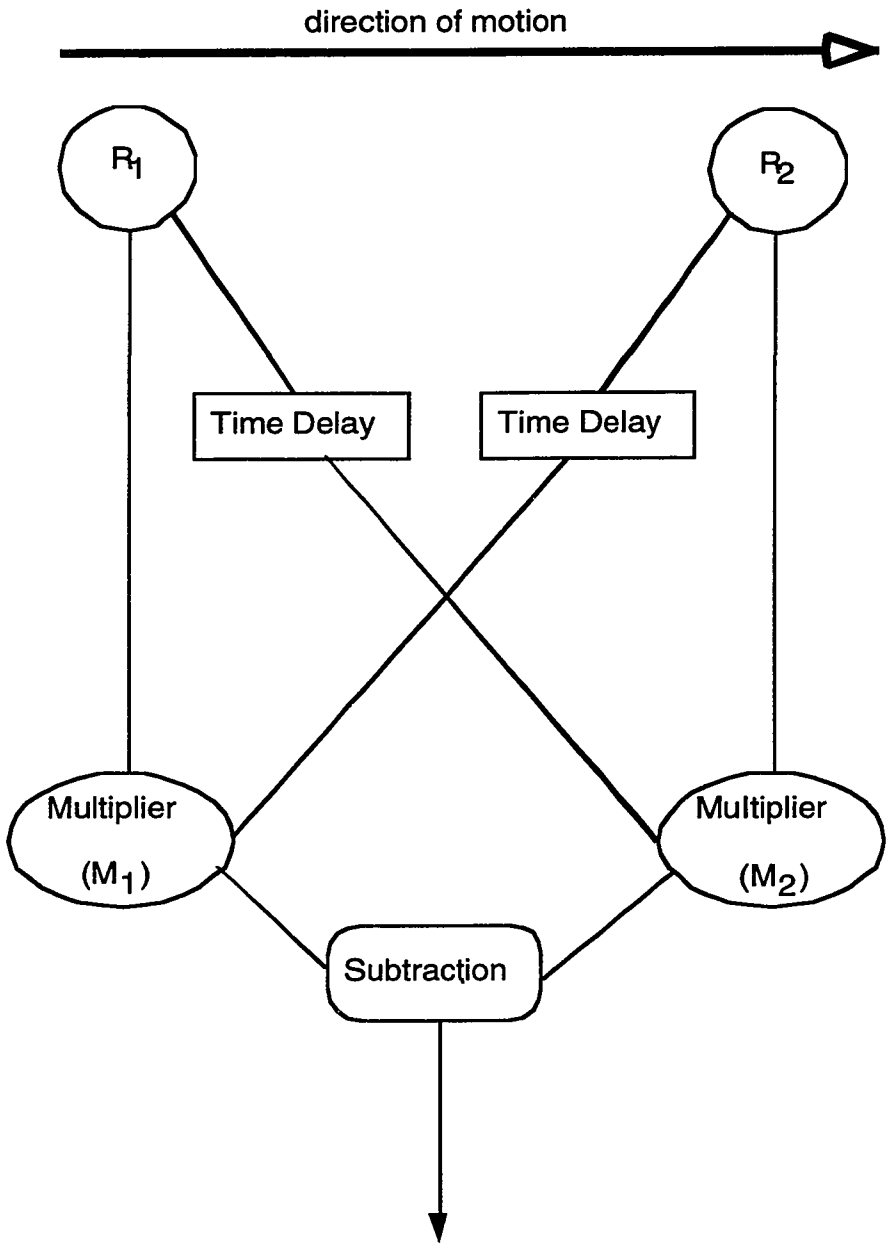

Figure 2. Schematic of the classic Reichardt detector. Two subunits tuned to motion in opposite directions provide an opponent motion detector which is better able to distinguish motion from non-motion phenomena than the individual subunits.

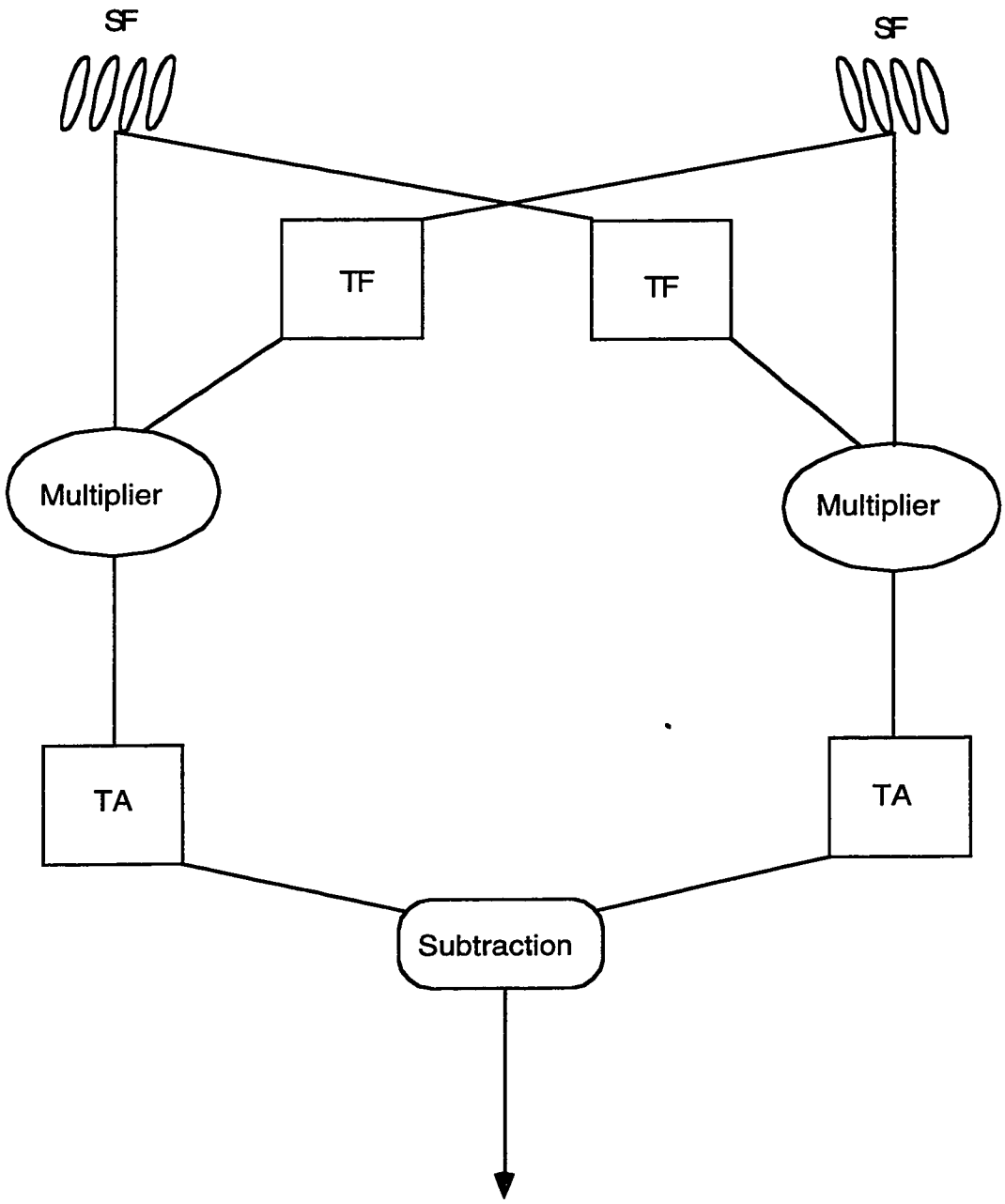

Figure 3. Schematic of the elaborated Reichardt detector. Subunit input is first fed into a spatiotemporal filter (SF) and then a linear time filter (TF). The two subunit signals are then multiplied before being correlated by a time averaging operation (TA). Lastly, the subunit outputs are subtracted to yield the ERD output.

elaborated version of the Watson and Ahumada (1985) model and the Adelson and Bergen (1985) model have been shown to produce equivalent outputs to the ERD (van Santen and Sperling, 1985) although the order of operations differs in the three models.

It is widely accepted that FO motion can be detected by using motion energy in the image as input to the conventional Reichardt detector described above. As previously mentioned, Chubb and Sperling (1988) argued that Fourier stimuli contain luminance contours oriented in space and time which give rise to energy that can be extracted by Fourier based motion detectors. If the image motion does not contain luminance contours oriented in space and time then the stimulus will be invisible to Fourier based motion detectors. SO motion is readily detected by the observer (Cavanagh & Mather, 1989) but the visual process by which SO motion is encoded has remained in contention. FO detectors would show ambiguous responses to SO stimuli because the motion energy in these stimuli is drift balanced, that is, the motion energy is equal in opposite directions, even after spatiotemporal filtering by the visual system (Chubb & Sperling, 1988).

The fact that it is not possible to extract SO motion from conventional FO motion detectors has led to the proposal that two distinct mechanisms are required for processing FO and SO stimuli. Methods suggested to encode SO motions include high-level feature matching (Ledgeway & Smith, 1994) and post-attentive object tracking (Cavanagh, 1992). The SO motion mechanism appears to operate more slowly than the FO system because longer stimulus durations are required to discriminate motion features such as direction of motion (Cropper & Derrington, 1994; Derrington, Badcock, & Henning, 1993).

Although the slower operation of the SO mechanism may be due to the fact that the SO system must analyze the spatial structure of the image before motion analysis can begin (Cavanagh & Mather, 1989), this does not appear to be the most logical explanation. Beat stimuli refer to SO stimuli formed by the addition of two sinusoidal gratings that differ in spatial frequency that show a periodic variation in contrast that is visible as a "beat" pattern.

Beat stimuli can be detected even at short stimulus durations at which motion direction is indiscriminable. This suggests that motion detection is what slows down the detection of SO motion direction rather than detection of spatial structure of the image (Derrington et al., 1993).

The distinction between FO and SO motion is not just a theoretical one. A number of empirical results suggest that FO and SO motion may be mediated by different mechanisms. For example, in contrast to FO stimuli, SO stimuli do not evoke optokinetic nystagmus (Harris & Smith, 1992), nor do SO stimuli permit the recovery of 3-D structure from 2-D motion images, a phenomenon called the kinetic depth effect (Dosher, Landy & Sperling, 1989; Landy, Dosher, Sperling, & Perkins 1991), unless the display contains only a small number of moving features (Prazdny, 1986). Also, SO stimuli produce weak or nonexistent (Derrington & Badcock, 1985; Nashida, Ashida, & Sato, 1994) MAEs to static test stimuli which is not the case for FO stimuli.

Other results support the idea of two separate but qualitatively similar motion systems. Mather & West (1993) demonstrated similar direction discrimination functions in response to SO versus FO motion stimuli. Detection thresholds for contrast modulations and motion direction show similar variations in response to manipulations of drift speed and eccentricity of FO and SO motion stimuli (Smith, Hess, and Baker, 1994). Neither FO nor SO mechanisms are capable of providing very reliable signals in response to plaid patterns of high spatial frequencies (Derrington, Badcock, & Holroyd, 1992).

If SO and FO mechanisms work according to similar principles, there may be some interaction between the mechanisms (Derrington & Badcock, 1985). Previous research has reported effects consistent with the combined effects of FO and SO responses such as in the case of direction specific adaptation (DSA). After exposure to an adapting stimulus moving continuously in one direction (for example, rightward), DSA occurs when the detection threshold for a test stimulus moving in the same direction (rightward) is elevated relative to a stimulus moving in the opposite (leftward) direction. DSA and direction

specific cross-adaptation has been reported for FO and SO stimulus types (McCarthy, 1993; Turano, 1991). Based on the study of plaid patterns that move in discrete jumps rather than smoothly, Derrington, Badcock, and Holroyd (1992) indicated that there is a trade-off between the FO and SO mechanisms. The plaid patterns they used were configured so that the FO components of the plaid would jump at the same rate as the plaid envelope but the SO components would only jump by 1/2 the rate of the FO components. Theoretically for jump sizes of 1/4 period of the envelope of the plaid, a SO mechanism signal would give rise to an ambiguous motion percept and the ability to detect the plaid direction should be at chance levels. However, their subjects' responses indicated that the plaid direction detection levels were much greater than chance at jump sizes of 1/4 period. This suggests that under conditions where the SO motion system is at a disadvantage, the FO system may predominate in order to reduce motion ambiguity.

Not all researchers agree that FO and SO motions are encoded by separate motion mechanisms. FO and SO stimuli may contain elements in common which could be processed by a common mechanism in the motion pathway or FO and SO signals may involve an interaction between mechanisms (Wilson et al., 1992) at a higher level in the visual pathway. Chubb and Sperling (1988) pointed out that in some cases SO motion can be encoded by energy-based processes if the motion signal of the stimulus is first nonlinearly transformed (e.g. rectified) and then passed through the appropriate spatial and temporal filters. That is, there is no need to resort to a theory of feature tracking to explain SO motion (Smith, 1994). Grzywacz (1992) suggested that both FO and SO motions could be detected by a common mechanism composed of a rectified band-pass filter in front of a ME filter (Chubb & Sperling, 1988). One possibility is that both FO and SO stimuli contain common elements which could be processed by one low-level mechanism. For example, Smith & Ledgeway (1997) argued that many of the SO stimuli used in experiments to test the FO versus SO distinction may contain FO artifacts which could be used by a FO system to detect motion. However, the fact that SO stimuli cannot elicit

certain visual phenomena which are elicited by FO stimuli provides evidence against the viability of one common low-level motion mechanism.

The kinetic depth effect (KDE) can be driven by both FO and SO stimuli but the effect is not very robust in response to complex SO stimuli such as luminous tokens moving on a less luminous background where the contrast polarity of the tokens is alternated (Landy et al., 1991). However, the KDE does produce a clear perception of motion for simple SO stimuli such as the dynamic noise on static noise background displays representing simple wire forms used by Prazdny (1986). It is possible that the SO system was intended only to enhance the functioning of the FO system by providing additional input into the process. Landy et al. (1991) suggested that even though the SO motion mechanism is weak, low in spatial resolution, and concentrated at the fovea, there are some indications that SO mechanisms provide input into the shape computations of the KDE.

Albright (1992) described cells in area MT of monkeys which supported the idea that SO stimuli are less salient for the visual system than FO stimuli. Although Albright found that many of the MT cells acted as generalized motion detectors in that they respond to both FO and SO motions, SO stimuli elicited similar but weaker responses than FO stimuli. However, these effects could be equated if the contrast of the FO stimuli was reduced. If one stimulus provides only weak input to the visual system, its "salience" may be reduced when the two stimulus types are presented together. This might explain the chance-level direction discrimination performance in the Mather and West (1993) study in which subjects were asked to detect apparent motion in kinomatograms where the frames alternated between texture-defined blocks (SO) and intensity-defined dots (FO) of equal contrast. For kinematograms where both frames contained only one of the stimulus types, direction discrimination performance was a function of displacement size.

Smith (1994) promoted the existence of three motion-detection mechanisms in human vision, an intensity based mechanism sensitive only to FO motion, an intensity

mechanism involving a nonlinear transformation of the luminance profile of the image so that the mechanism is sensitive to SO motion, and a third feature tracking mechanism that can detect both stimulus types. Smith suggested that SO stimuli may be processed by two discrete mechanisms because he demonstrated that SO stimuli can be perceived based on the principles of either a feature-matching theory or an energy theory depending upon the viewing conditions. In Smith's experiments, the energy system was dominant but the feature based process took over when the energy system was disabled.

Whether or not FO and SO stimuli are processed by separate mechanisms, it is clear that these two stimulus types do not give rise to identical motion percepts in all cases. Dosher, Landy, and Sperling (1989) demonstrated that SO motions were unable to support the KDE. In the continuation of these KDE experiments, Landy et al. (1991) supported the idea that SO motions can contribute to the KDE even though SO motions alone may not be able to support the KDE. On the other hand, Prazdny (1986) was able to demonstrate KDE in response to SO motions when the stimuli simulated simple wire-frame objects. These results raise questions about the involvement of SO motions in depth computations. These questions are similar to those raised by Livingstone and Hubel (1988) concerning the role of chromatic signals in the recovery of 3-D structure. The purpose of this research study is to address whether SO stimuli can induce a phenomenon which requires the perception of motion in depth, the vection illusion.

Vection

A major problem for the visual system is the discrimination between passive locomotion and object motion because objects in motion relative to the stationary observer may generate similar or identical optic flow patterns to the flow patterns generated during passive transport of the observer. During active movement, interacting sensory subsystems including the skeletal and muscular, vestibular, visual, cutaneous, and kinesthetic subsystems work together to produce a signal indicative of self-motion of the

individual (Johansson, 1977). When the individual moves about in the environment in an active way such as during walking or running, there is corroborating information available from a number of sensory subsystems upon which to interpret the motion experience. Lishman and Lee (1973) demonstrated that vision plays a dominant role in the subsystem complex.

If an individual is passively transported under conditions of acceleration or rotation with respect to the earth, the self-motion signal arises mainly from visual and vestibular input. Under these conditions, the motion signal relies heavily on the acceleration signal arising from the vestibular input (Johansson, 1977). The visual input merely serves to supplement the vestibular inputs in self-motion perception. Physiological evidence of this phenomenon is demonstrated by cells in the vestibular nuclei which respond to visual motion in one direction and to vestibular signals arising from body rotation in the opposite direction (Howard and Heckman, 1989).

The situation becomes more complicated when an individual is transported under conditions of constant velocity. The laws of physics indicate that the states of rest and uniform linear motion (that is, at zero acceleration) are mechanically indistinguishable. While the presence or absence of flow in the visual field may help the observer to distinguish between these two states, visual flow may serve to confuse the individual. Unlike vestibular stimuli which lead to a particular sensation of body motion, visual motion stimuli can result in two perceptual interpretations (Brandt, Dichgans, & Koenig,1973; Lishman & Lee, 1973. Egocentric motion perception occurs when observers perceive themselves as stationary while faced with a moving visual field. Exocentric motion perception occurs when observers perceive the moving surround as stable and see themselves as moving. Brandt et al. (1973) suggested that exocentric motion perception occurs when central nervous systems, which normally receive vestibular input, use visual input as a substitute to determine the observer's motion relative to the environment.

Illusory self-motion or vection occurs when an observer misinterprets motion in the visual field as a signal arising from self-motion (Telford & Frost, 1993; Anderson & Braunstein, 1985). Vection characteristically is an all-or-none phenomenon (Johansson, 1977) which may be perceived as indistinguishable from actual self-motion. Under natural circumstances, the input of certain subsystems, such as the vestibular and kinaesthetic subsystems, is reduced or unavailable when an observer is towed through the environment without any active movement on the part of the observer. This can partially explain the vection illusion, that is, vection occurs in the absence of sensory signals to oppose the interpretation of the visual flow as arising from self-motion. In the case of passive transport under conditions where no acceleration occurs, the vestibular system provides only a weak response. Therefore, the visual input is the dominant factor used to signal self-motion relative to the environment.

Vection occurs when the observer is stationary, a circumstance which produces similar sensory input to conditions of zero acceleration. That is, there is no sensory input provided to the vestibular system and visual input alone is used to determine whether the observer is moving through the environment. The visual system may have a role in suppressing vestibular processing during the vection experience. Conversely, the active vestibular system may play a role in restraining the vection illusion as suggested by the fact that greater vection magnitudes normally are evoked in stimuli which simulate motion about an axis which is not expected to stimulate the otoliths (Telford & Frost, 1993). The fact that certain subjects experience motion sickness in response to vection stimuli suggests that visually induced self-motion interacts with vestibular processing (Anderson & Braunstein, 1985).

As vestibular processing provides information to indicate that either the observer is not moving or the observer is travelling at a constant speed, it suggests that, in certain cases, a sensory ambiguity must be overcome in order to experience vection. Johansson (1977) suggested that the subjects who cannot resolve this sensory ambiguity will not

experience vection. This finding was supported when all subjects reported self-motion under conditions where the total visual field was covered by moving stimuli and conflicting signals were minimized (Brandt et al., 1973; Johansson, 1977). In all cases, the vection stimulus is initially seen as object motion before the interpretation switches to self-motion.

A distinction is usually made between three types of illusory self-motion: 1) Linear vection refers to the perception of self-motion in a linear direction that often occurs along the line of sight (Telford & Frost, 1993). For example, Lishman and Lee (1975) used linear vection to make their subjects believe they were on a moving trolley in a set-up where the walls could be moved independently of the floor. 2) Circular vection refers to a sensation of turning (Howard & Heckman, 1989). To induce circular vection, a drum with alternating black and white stripes is rotated around a stationary subject (Brandt et al., 1973). 3) Curvilinear vection corresponds to the impression of taking a bend (Sauvan & Bonnet, 1993). This type of vection corresponds to an experience such as turning a corner in a vehicle.

In response to non-competing motion signals, the illusion is always perceived in the direction opposite to the direction of visual stimulation (Dichgans and Brandt, 1978). Telford, Spratley, and Frost (1992) demonstrated that for stimuli composed of component motion signals of opposing directions, vection strength is not reduced but the perceived direction of self-motion may be related to the relative depth cues in the stimulus. They compared displays with the center and surround moving in opposite directions versus wide angle displays using only one motion direction and found that vection strength as measured by latency to onset and tracking speed was not significantly different for the two displays. However, the direction of the vection experienced was determined by the portion of the display which was perceived as being the more distant.

Other psychophysical evidence supports the idea that vection is produced by the more distant of two superimposed visual displays. For example, Brandt, Wist, and Dichgans (1975), observed a weaker vection response to stereoscopic displays where

stationary bars were made to appear behind a moving display but not when the bars appeared to be in front of the moving display. It is the display which appears more distant rather than the display which is actually more distant which influences the vection response (Howard & Heckman, 1989; Ohmi, Howard, & Landolt, 1987; Telford et al., 1992) regardless of whether the observer fixates on the near plane or the far plane (Heckman & Howard, 1991). Ohmi et al. (1987) found that subjects shown depth displays presented monocularly as two superimposed images at the same distance as for binocular presentations indicated that the depth relationship reversed periodically along with a corresponding reversal of the vection direction.

One clue the visual system can use to make the discrimination between object and self-motion is the image flow pattern in the visual display. Movement of the observer often generates a continuous flow of visual information over the whole retina while object motion often results in local flow information overlaid on the total flow of a stationary environment. However, this general rule does not always hold true such as when the only available movement information to the observer is through the window of a vehicle moving linearly and at a constant speed (Johansson, 1977).

Another clue the visual system may use to determine whether the observer is in fact moving is the perceived depth in the display. Anderson and Braunstein (1985) found a correspondence between subjects' ratings of perceived depth and strength of the vection experience in response to stimuli in the central visual field. When this finding did not hold for increased display sizes, Anderson and Braunstein (1985) suggested that the motion in the periphery of their displays interfered with perceived depth information contained in the central region of the display.

Factors such as the size, eccentricity, and speed of the stimulus have been reported to influence the vection experience. Vection magnitude has consistently been reported to correlate with the total area of the inducing stimulus area (Brandt et al., 1973; Post, 1988; Telford et al., 1992) but the relationship between vection magnitude and stimulus

eccentricity is not as clear. Telford and Frost (1993) observed a reciprocal relation between vection strength and eccentricity. An increase in the retinal velocity of the stimulus increases the perceived speed of self-motion (Brandt et al., 1973).

Typically, vection is induced in response to large optical flow fields but the illusion can also be induced by the stimulation of select portions of the visual field. The vection experience has been demonstrated to occur in response to central visual field stimulation (Anderson & Braunstein, 1985; Anderson & Dyre, 1989) and peripheral visual field stimulation (Brandt et al., 1973; Dichgans & Brandt, 1978; Johannson, 1977). Initially it was believed that peripheral vision was primarily responsible for the vection experience and that stimulation of the central visual field was specialized for object motion (Dichgans & Brandt, 1978). However, this erroneous conclusion was based on studies which did not control for stimulus size or retinal location (Telford et al., 1992). Post (1988) found no difference in vection magnitude in response to stimuli of identical area which were presented either centered in the median sagittal plane of the subjects or 45 deg to the right of that location.

The reason why some of the early studies failed to demonstrate self-motion in response to central visual field stimuli may have been related to the displays used in the experiments. In the early studies, identical displays were presented in both the central and the peripheral fields. According to Anderson and Braunstein (1985), self-motion can be induced in response to either central or peripheral field stimulation but the type of stimulation necessary to induce vection in these regions differs. Retinal location and optic flow patterns may have been confounded (Stoffregen, 1985, as cited in Telford & Frost, 1993). In order for the motion signal to be consistent with natural vision images, the optical flow would have a lamellar structure in the peripheral field and a radial structure in the central field. Lamellar patterns contain elements that traverse the length of the visual field at constant velocity. Radial patterns expand outwardly from a central point and element velocity varies as a function of perceived depth. Telford and Frost (1993) found

that radial flow fields generated increased linear vection magnitude regardless of the retinal location which they ascribed to the internal depth structure in the images. In the lamellar displays all image elements were in the same simulated depth plane but in the radial displays the elements appeared in different simulated depth planes.

Using postural sway as an objective measure of the inducement of self-motion, Anderson and Dyre (1989) supported the importance of the central visual field in self-motion because there is greater sensitivity to motion and higher acuity in the central field as compared to the peripheral visual field. These researchers found that central visual field information could help the observer discriminate between self-motion and object motion in the environment. These advantages included the ability to make finely tuned postural adjustments, to determine the spatial layout of the environment and to detect changes in the orientation of the observer with respect to the environment with greater accuracy.

Physiology

Although the visual world is perceived as unified, the visual system breaks down the visual input into many different components, often arranged in hierarchical fashion. Visual system components that are selective for the patterns which occur during self-motion may not appear before the level of the medial superior temporal area (MST). However, inputs into the motion detection mechanism occur earlier in the visual system. The question remains as to how input received at the level of the retinal receptors is translated into a signal of self-motion.

Livingstone and Hubel (1988) reviewed the two major visual pathways originating from the retinal receptors, the parvocellular and magnocellular pathways. Although both pathways respond to motion stimuli to some extent, the magnocellular pathway (Figure 4) is primarily responsible for motion detection for middle and high velocity stimuli (Merigan and Maunsell, 1993). Anatomical and physiological studies of primate visual pathways indicate that the middle temporal cortex (MT) is important in motion encoding. MT

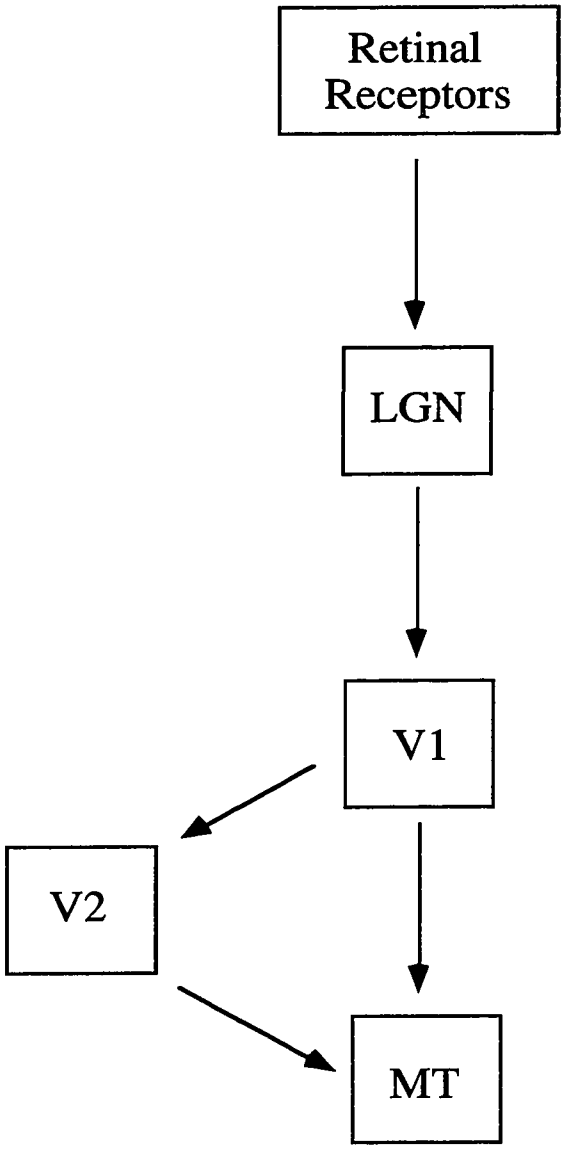

Figure 4. Schematic of the magnocellular pathway in the visual system. Area MT which is important for motion encoding receives most of its input directly from the striate cortex (area V1) but it also receives input indirectly via area V2.

receives most of its input directly from the striate cortex (area V1) but it also receives input from V2, the second visual area of the cortex (DeYoe and Van Essen, 1985). Wilson et al. (1992) postulated that the direct motion pathway accounts for the detection of first-order stimuli and the indirect pathway accounts for the detection of second-order stimuli.

Wilson et al. (1992) proposed a model that combined the responses of the FO and SO motion pathways to explain the perceived direction of moving 2-D patterns. That is, the two motion pathways may be independent at lower stages of the visual processing pathway but as the visual signal moves up the pathway to the level of area MT the outputs of the lower two motion pathways are combined to provide input into the next stage of the visual processing system. Single cell recordings have shown the existence of neurons in area MT (Albright, 1992) and other areas (Zhou & Baker, 1993) in the visual pathway which respond to the motion of both FO and SO motion.

A good candidate for the next step in the mechanism to encode vection is area MST. Area MT has direct projections to MST. Although no causal link has been established between MST and self-motion estimation, Perrone & Stone (1994) developed a model of self-motion estimation which suggests that image motion is first processed by MT type cells before the information is integrated in MST.

Duffy and Wurtz (1991a, 1991b) studied motion selective neurons in the dorsomedial region of the medial superior temporal area (MSTd). These neurons were directionally selective for moving visual images, preferred the stimulation of large visual flow fields, and responded to flow fields produced by different motion patterns such as rotating, expanding, or translational patterns of optic flow. These characteristics suggest that the MSTd cells are appropriate for the analysis of optic flow fields generated as an observer moves through the environment or as the environment moves with respect to the observer. As the vection illusion relies on the perception of self-motion, MSTd cells may play a role in vection induction.

In light of the information given above, one can speculate that separate visual pathways are initially required for the detection of FO and SO motions. FO motions appear to be detected in a direct pathway from V1 to MT. An indirect pathway from V1 to V2 to MT may account for the detection of SO motions. Wilson et al. (1992) proposed that the outputs of these two mechanisms are combined at area MT and there is physiological evidence to support this proposal. The question arises then as to whether neurons responsive to second-order motions at area MT or at lower levels in the visual pathway can provide input to propel the neurons in the MSTd which are involved in self-motion perception.

MAE

As mentioned before, MAE refers to phenomena where extended viewing of a unidirectional moving pattern results in an illusion of motion if the pattern subsequently stops drifting. Normally the perceived direction of the MAE is opposite to the direction of the adapting pattern. It has been generally assumed that MAE is the result of adaptation of motion-sensitive components in the visual system. MAE has a long history dating back to at least the time of Aristotle but it was first reported scientifically by Addams in 1834 (as cited in Wade, 1994). MAEs have been used extensively in vision experiments as a tool to explore the organization of the visual system (Verstraten, Fredericksen, Van Wezel, Lankheet, & Van de Grind, 1995) and to provide a link between psychophysics and physiology (Wade, 1994).

FO and SO motions have been studied in relation to their effects on the MAE and certain distinctions have emerged. For example, MAE with static test patterns is strongly induced by FO motions but only slightly or not at all by SO motions (Derrington & Badcock, 1985; Nishida & Sato, 1995) whereas MAE with dynamic test patterns is strongly induced by both FO and SO adapting motions (Nishida & Sato, 1993). Nishida

and Sato (1994) used the relationship between the two MAE types and FO and SO motion to suggested that different motion mechanisms may underlie static and dynamic MAEs. According to Nishida, Ashida, and Sato (1994), static MAE reflects the operation of a lower-level motion system used predominantly in the processing of FO signals while dynamic MAE reflects the operation of a higher-level motion system that can process both FO and SO signals. Considering that MAE shows big differences in response to FO and SO signals, MAE may be useful as a comparison for the effects of FO versus SO motions on vection perception.

FO and SO stimuli differ in their ability to induce static MAE (Nishida et al., 1994) and the kinetic depth effect (Dosher et al., 1989; Landy et al., 1991) despite the fact that both stimulus types can induce certain phenomena such as direction specific adaptation (McCarthy, 1993; Turano, 1991). FO and SO motions may subserve different visual functions. Therefore it is possible that in contrast to FO motion, SO motion stimuli may be unable to support visual functioning related to depth perception except in the case of simple visual patterns (Prazdny, 1986).

Vection is a "behavior" induced by optic flow patterns. The KDE and vection share their dependence on image flow requirements to produce an illusion of 3-D motion but the visual input required for vection may be simpler. The optic flow patterns used to drive vection can be composed of images where the image velocity remains constant at a point as opposed to the complex stimuli used by Landy et al. (1991) to examine the KDE which had image velocities that changed over time at each retinal position. Prazdny (1986) demonstrated that SO motions permit the recovery of 3-D structure from motion if the motion stimuli depict very simple forms. Therefore, it is possible that SO motion signals can support vection and yet be inadequate to support the recovery of complex 3-D structure from motion.

To evaluate this possibility, a series of three experiments examined the induction of vection and MAEs by patterns with fixed velocity at each image point. Two questions were of particular interest: 1) Can SO stimuli support the vection illusion?, and 2) Are vection and MAE similarly affected by the FO/SO distinction?

General explanation of the stimuli used in Experiments 1 and 2 to test the influence of FO and SO motions on vection and MAE

Radial expansion patterns were chosen as the vection stimuli because flow fields of this type have been shown to induce self-motion along the line of sight (Anderson & Braunstein, 1985; Ohmi & Howard, 1988; Telford & Frost, 1993). All the experimental stimuli approximated forward linear motion through a cylindrical tunnel whose walls were shaded in the form of a sinusoidal grating. The mathematical definition of the basic vection stimulus (i.e., the radial expansion pattern) is given by equation 1:

$$\mathbf{V}(x, y, t) = \sin(2\pi c / d + 2\pi\omega t) \qquad (1)$$

where c represents a constant related to the spatial frequency of the pattern, $d = (x^2 + y^2)^{-1/2}$ represents the distance from the origin of the image, c / d is the spatial frequency of the image at d, t represents time, and ω represents the temporal frequency. The spatial frequency of $\mathbf{V}(x, y, t)$ decreases as a function of the distance from the origin, d. The temporal frequency, ω, was fixed at 3 Hz. Thus, the instantaneous velocity increased as a function of d. $\mathbf{V}(x, y, t)$ takes on the values [-1,1].

From Equation 1, one can derive a conventional FO vection stimulus having the form

$$\mathbf{S}_o(x, y, t) = \mu + \alpha\,\mathbf{V}(x, y, t) \qquad (2)$$

where α is the amplitude of the mean-zero vection signal, and μ, the mean luminance is chosen so that $\mathbf{S}_o(x, y, t) \geq 0$. Figure 5 presents a static image of the stimulus described in

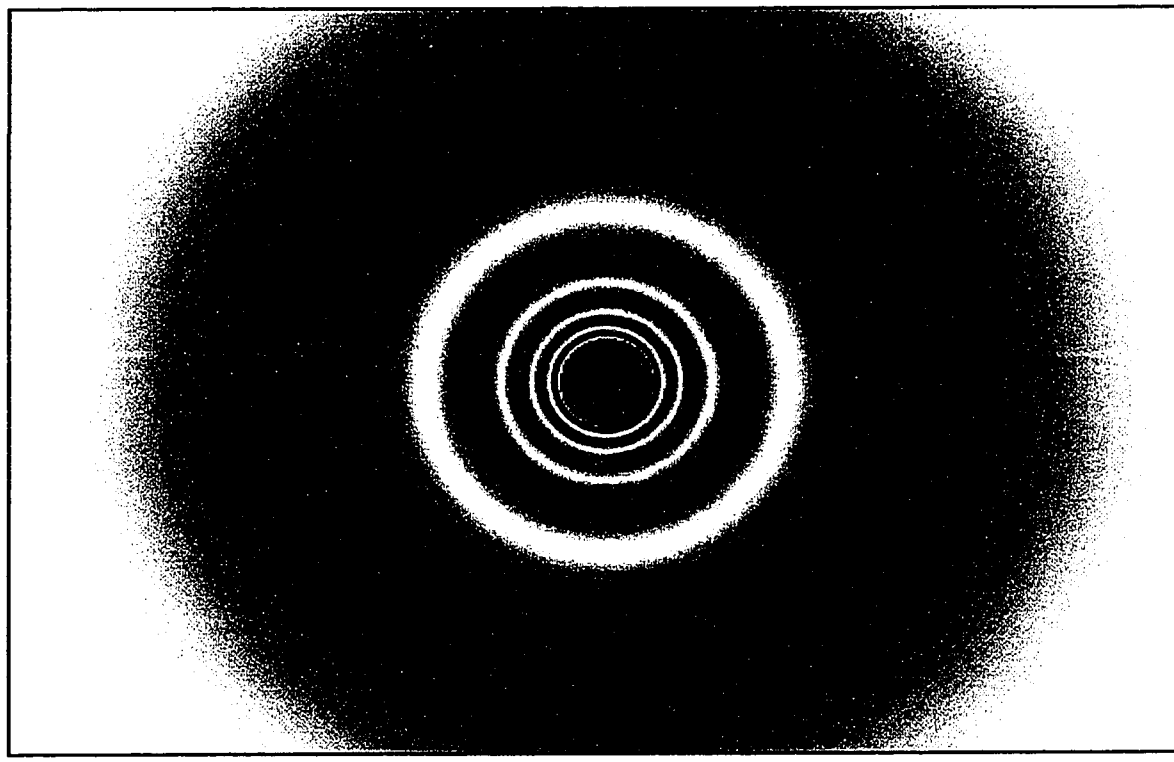

Figure 5. **V**, the basic vection signal.

Equation 2. This stimulus, which served as the control stimulus for the experiments reported here, is the visual image of a forward linear path through a cylindrical tunnel with walls "painted" in the design of a sinusoidal grating.

Carrier Signals and Contrast Envelopes

To create a larger class of vection stimuli, the basic vection stimulus in Equation 1 was used as a contrast envelope which modulated the amplitude of a carrier signal. The modulating contrast envelope has the form

$$\mathbf{M}\ (x,\ y,\ t) = 1.0 + \mathbf{V}\ (x,\ y,\ t) \qquad (3)$$

where $\mathbf{V}\ (x,\ y,\ t)$ is the mean-zero vection signal from Equation 1; $\mathbf{M}\ (x,\ y,\ t)$ takes on the values [0,2].

Three different carriers were used which will be referred to as the concentric, noise and radial patterns. Examples are shown in Figure 6. The carrier patterns can generally be described as

$$\mathbf{C}\ (x,\ y,\ t) = n + \mathbf{D}(x,\ y,\ t) \qquad (4)$$

where **D** (x, y, t) is one of the carrier patterns, each of which was mean-zero with values ranging from $n = 1$ to -1, and n is the mean of $\mathbf{C}\ (x,\ y,\ t)$.

The concentric carrier (Figure 6a) had the same form as V but its spatial frequency was three times higher. The radial carrier (Figure 6b) portrays a tunnel with constant intensity lines, with a sinusoidal cross-section of the 64 cycles, running through the tunnel. The third carrier was random noise (Figure 6c) with a check size of 2 x 2 pixels. The intensities in the noise carrier were drawn from the distribution sin(u), where u is a random

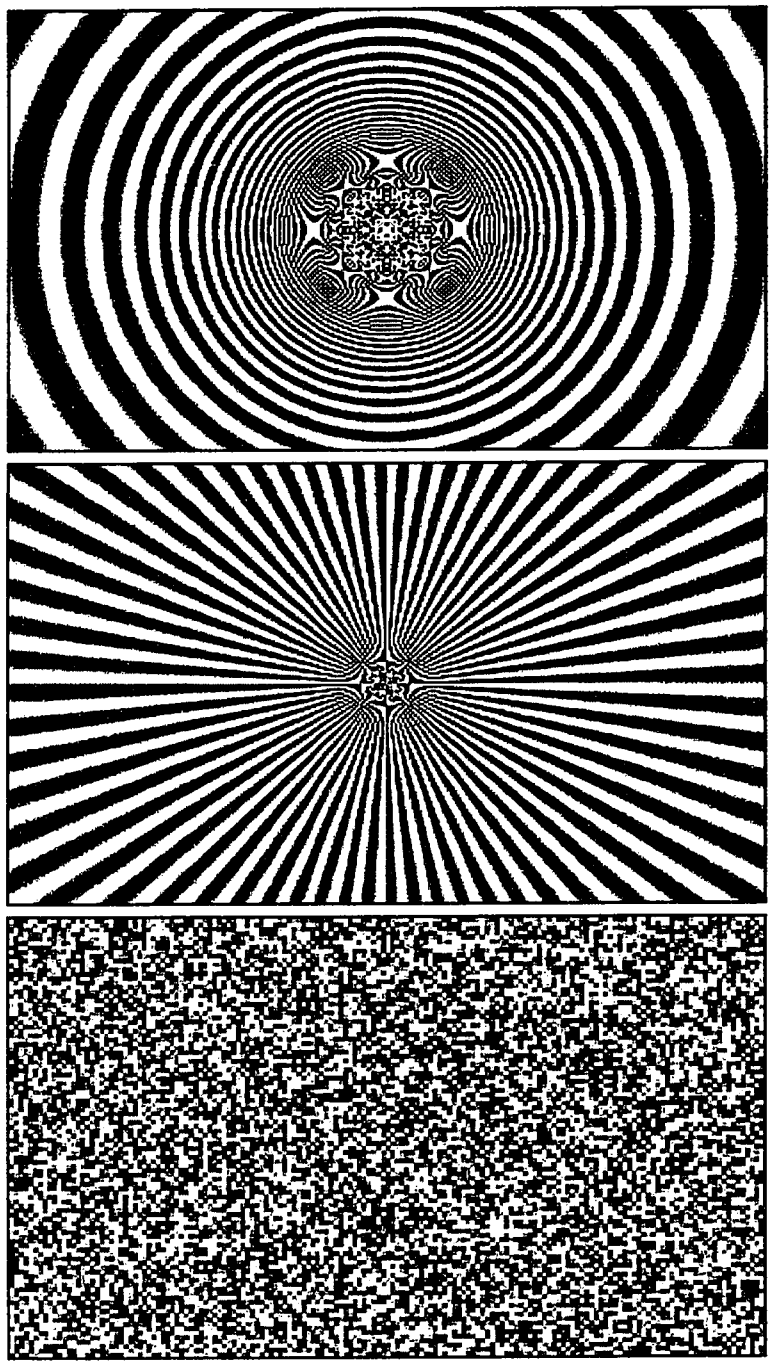

Figure 6. Three static carriers were combined with the basic motion signal, **V**, to create the MAE and vection stimuli used in the experiments. Three sequences were created using different carriers. The concentric carrier (a) had the same form as **V** but its spatial frequency was three times higher. The radial carrier (b) is a sinusoidal function of angle which goes through 64 cycles per 360 degrees. The third carrier was quasi-random noise (c).

variable between 0 and 2π.

Combining the Modulator and the Carrier

The carriers and the modulator were multiplied to yield stimuli of the form

$$\mathbf{S}\ (x,\ y,\ t)\ = \mu + \alpha \mathrm{M}\ (x,\ y,\ t)\ \mathbf{C}\ (x,\ y,\ t) \qquad (5)$$

The constant μ was chosen so that $S\ (x, y, t) \geq 0$. The constant α was used to control the average contrast of the stimulus. The value of α was set to 0.3 fL and the value of μ was set to 1.33 fL in Experiments 1 and 2. In Experiment 3, the value of α was set to 0.6 fL and the value of μ was set to 2.33 fL. To examine the form of the stimuli in greater detail, Equation 5 can be expanded using equations 2 and 3 [the space and time indices (x, y, t) have been removed to increase legibility]:

$$\mathbf{S} = \mu + \alpha\ (1.0 + \mathbf{V})(n + \mathbf{D}) = (\mu + \alpha n) + \alpha n\mathbf{V} + \alpha\mathbf{D} + \alpha\mathbf{VD} \qquad (6)$$

It can be seen from Equation 6 that the stimuli contain four terms: a constant, a term representing the basic vection signal, a term representing the carrier pattern, and a term representing the product of the vection signal and the carrier pattern. The explicit presence of local components of the vection signal **V** depends upon the value of *n*.

The Effect of Varying *n*

The constant *n* has a critical effect on the properties of the stimuli in Equation 6. When $n = 0$ Equation 6 reduces to

$$\mathbf{S} = \mu + \alpha\mathbf{D} + \alpha\mathbf{VD} \qquad (7)$$

The vection signal, **V**, exists only in combination with the carrier term, **D**, as part of the product derived in the last term of equation 7 so that the local Fourier components of **V** are not explicitly present in **S**. When $n = 1$, the value of **C** is greater than or equal to zero and **V** then occurs explicitly as one of the additive terms contributing to stimulus **S**. That is, when $n = 0$ the local Fourier components of **V** are not explicitly present in the stimulus and when $n \neq 0$ the local Fourier components of **V** are explicitly present in the stimulus. It should be noted that the elimination of the Fourier components of **V** does not by itself yield a non-Fourier stimulus. It also depends on the carrier with which **V** is combined. A case in point is the radial display. Local Fourier components can be eliminated in the multiplicative combination of the radial carrier with the modulator but this stimulus has no non-Fourier representation in the spatiotemporal domain. Any spatiotemporal analysis of a one dimensional slice of the image starting from the center of the stimulus results in an average luminance level which is greater than zero.

Figure 7 presents nine stimuli used in Experiments 1 and 2. Each carrier was combined multiplicatively with the vection signal, using three values of *n*.

The mean of **S** varies with *n*. The contrast of **S** also changes with *n* but the exact nature of this change depends on how contrast is defined. Using the standard Michelson contrast

$$C = (L_{max} - L_{min})/(L_{max} + L_{min}) \qquad (8)$$

where L_{max} and L_{min} refer to the highest (peak) and lowest (trough) pixel intensities respectively, contrast is inversely related to *n*. A measure of the depth of the contrast modulation is given by

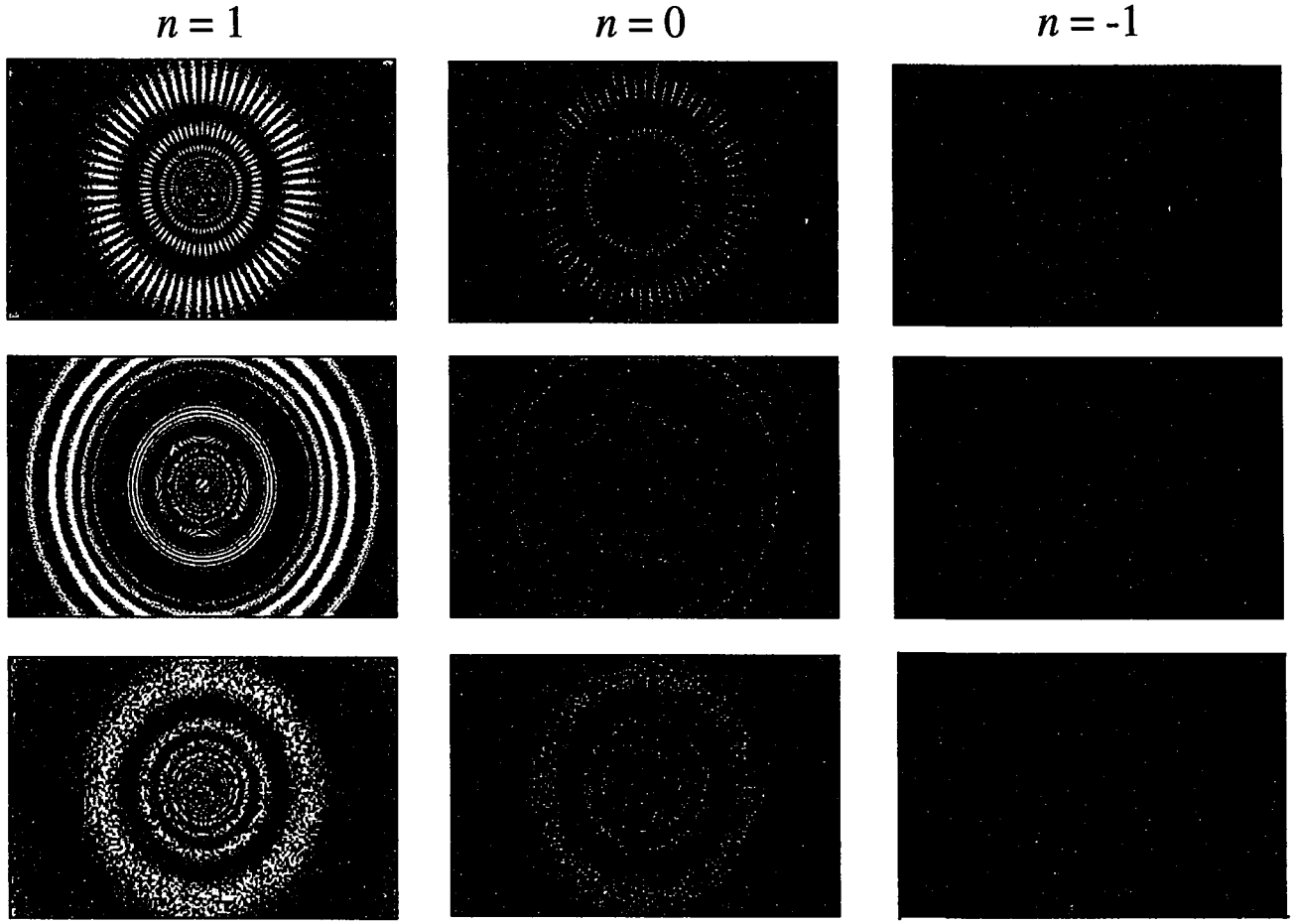

Figure 7. Examples of the stimuli used in Experiments 1 and 2. Each panel represents the multiplicative combination of **V** (*x, y, t*) with the radial, concentric, or noise carrier for $n = -1, 0$, and 1. The Fourier components of **V** (d, t) are present in for images where $n \neq 0$. The mean luminance is lowest for $n = -1$, intermediate for $n = 0$, and highest for $n = 1$.

$$M = (C_{max} - C_{min})/ (C_{max} + C_{min}) \quad (9)$$

where C_{max} and C_{min} refer to the maximum and minimum contrasts in the image (as defined by equation 8). This measure is not informative for the contrast modulation because M = 1 for all values of n ($C_{min} = 0$ irrespective of n).

The luminance profiles of the images also varied with n., as can be shown by the schematic of the luminance profile of the noise stimulus in Figure 8.

An important question is how variations in n value affect the ME mechanism used to detect FO and SO signals. Based on the contrast modulated noise stimulus carriers with ($n = +1$ or -1) and without ($n = 0$) explicit Fourier components described above, Gurnsey, Fleet, and Potechin (1998) used a ME model to determine how ME mechanisms differ in response to n value in the FO and SO channels. The FO channel represented the operation of the ME mechanisms described above. The response of a SO channel was approximated using a non-linear transformation of the luminance values. Each spatial slice in the space-time representation of the signal was convolved with a small center-surround filter and the results were half-wave rectified. The ME mechanism was then applied to the rectified filter responses. The effects of varying n value were evident in the FO channel analysis. That is, a sizable amount of ME is eliminated from the signal in the FO channel when $n = 0$. Conversely, the approximated SO channel was relatively unaffected by changes in n value.

Unique Qualities of the Radial Carrier

Although all three carriers are static images, only the radial carrier is consistent with the image flow observed during self-motion. If an observer moved through a tunnel with walls drawn as for the radial carrier, no motion would be detected if the observer traveled without a change in role, pitch, or yaw (rotation about the x, y, and z axes with respect to the center of gravity of the observer). For this reason, modulating the radial carrier (Figure

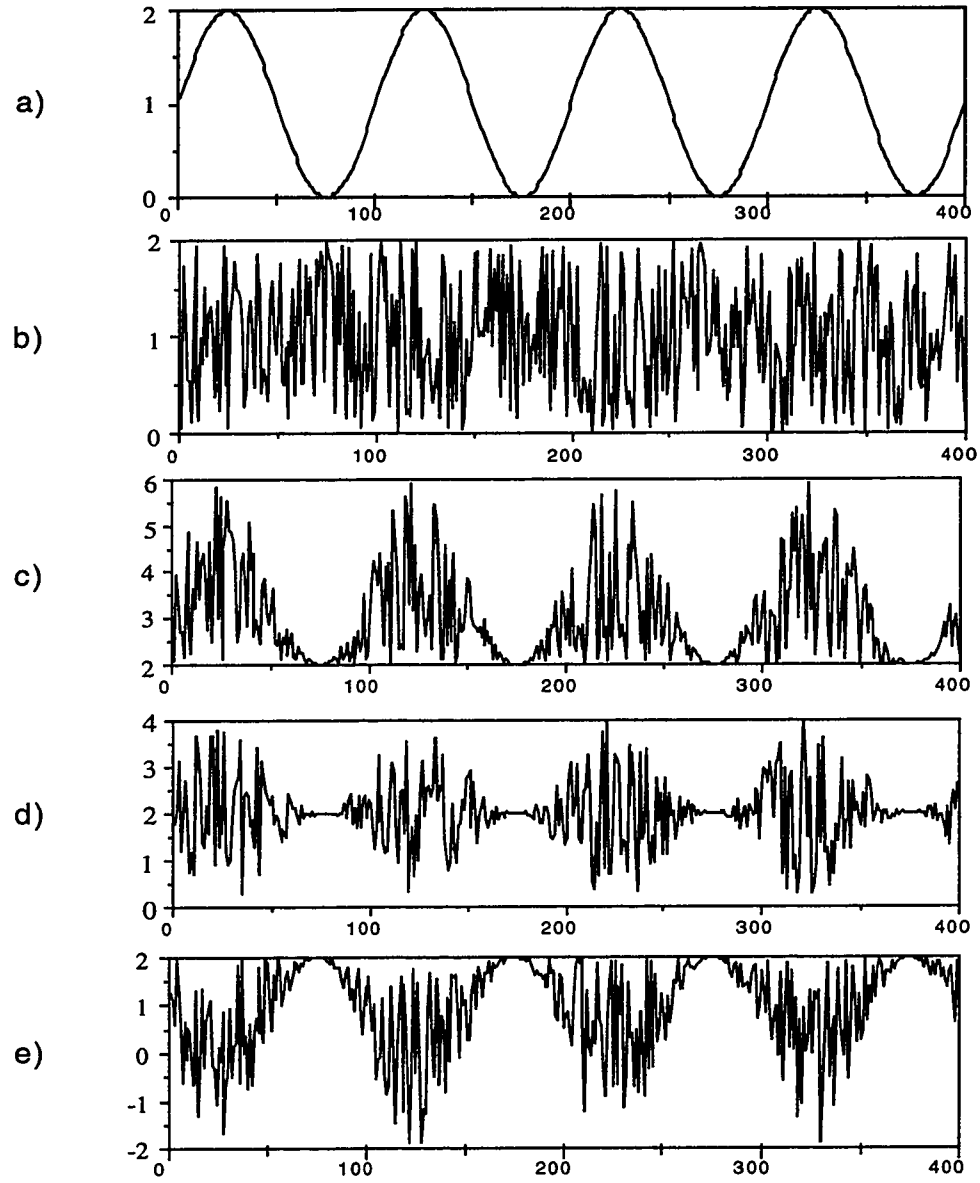

Figure 8. Luminance profiles of the noise stimuli and the components used to make them. Each trace represents a horizontal section through the image and indicates the luminance changes as a function of spatial position. The noise stimuli were produced by the multiplication of a sine wave grating (a) and a quasi-random noise carrier (b). The resultant image was luminance modulated at $n = 1$ or -1 (c or e) and contrast modulated at $n = 0$ (d).

6c) produces a motion signal which is consistent with self-motion through a tunnel. The concentric and the noise carriers are inconsistent with natural image flow produced as the observer nears an object because they remain static while the motion signal expands. It has been demonstrated that the presence of a stationary textured background can cause a decrease in MAE (Smith, Musselwhite and Hammond, 1984) and vection (Brandt et al., 1975) strength. However, Smith et al. (1984) reported that MAE could be enhanced if all motion elements in the display moved in the same direction. As the motion signal of the radial carrier would not appear differently if the radial carrier was moved outward relative to the origin, all elements in the radial display may be interpreted as moving in the same direction. Therefore, it would be expected that the noise and concentric carriers would reduce vection and MAE strength because it is apparent that these carriers are not in motion. On the other hand, the radial carrier may not affect or may even serve to increase vection and MAE strength because there is no information in the motion signal to contradict the perception that the radial carrier is moving along with the modulator.

Mather and West (1993) indicated that certain stimuli would not be considered to be SO stimuli although they could be called nonFourier. This is true in the case of the radial carrier. Although the radial stimulus could be considered to represent SO motion, the radial carrier differs from the other carriers in that it may not be considered nonFourier. Explicit Fourier components can be eliminated from the image when $n = 0$ but a one dimensional slice of the signal through the origin never yields a signal with an average luminance level equal to zero. In other words, the multiplicative combination of the radial carrier with **V** never produces a SO stimulus even when the local Fourier components have been eliminated from the motion signal. Therefore, the multiplicative combination of the radial carrier with **V** using different values of n may be thought of as different forms of a FO stimulus. At $n = 0$ the radial stimulus will contain less FO motion energy than for other values of n.

In summary, combining the three carriers with different values of n creates stimuli with different formal properties. When $n \neq 0$, local Fourier components of **V** are explicitly present in the motion signal, irrespective of carrier type. The radial carrier is consistent with the vection signal, **V**, while the concentric and noise carriers are not. Therefore the concentric and noise carriers may provide additive noise to the signal but the radial carrier combined multiplicatively with **V** would be expected to produce locally coherent (FO) motion. When $n = 0$, local Fourier components of **V** are not explicitly present in the motion signal, irrespective of carrier type. The multiplicative combination of the concentric and noise carriers with **V** results in standard SO motion signals. However, in the case of the radial carrier, the resulting signal produces locally coherent motion, even though the local FO components of **V** are not explicitly present in the stimulus.

EXPERIMENT 1

Although it has been established that motion can be perceived in SO stimuli, the SO mechanism may not support motion in depth as suggested by the fact that SO motions do not always support the KDE, an illusion that simulates motion in depth. However, if the SO motion mechanisms respond to visual flow in a manner similar to the FO channel, the SO motions may be expected to elicit vection. The purpose of Experiment 1 was to determine whether FO and SO motions differ in their ability to induce vection. The ability of FO and SO motions to elicit MAEs was also examined to determine whether there is an association or dissociation between FO and SO motions with respect to their abilities to induce vection and MAE.

Method

Subjects

Five subjects (three males, two females) participated in the experiment. All reported 20/20 or corrected to 20/20 vision. The subjects included one experienced psychophysical observer and four naive observers.

The Display

The stimuli were generated on and controlled by a PowerMac 7100/66 computer and were presented at a frame rate of 67 Hz. An INFocus Panel Book 550 display tablet combined with a Dukane projector was used to back-project the stimuli onto a 305 cm x 230 cm vinyl screen (CINEFLEX, rear-projection screen, Draper Shade & Screen, Spiceland, Indiana). Distortion products refer to luminance modulations which occur in contrast-modulated images that have been non-linearly transformed and which have the same waveform as the contrast modulation. The computer's CLUT was gamma corrected

to eliminate nonlinearities in the display which could introduce moving distortion products into the SO stimuli. Such distortion products are FO motions that SO stimuli are supposed to eliminate. Subjects viewed the screen, at a distance of 130 cm, from within an observation booth. The booth was intended to enhance the authenticity of the image flow as motion that arises from self-motion (Telford & Frost, 1993). An 84 cm x 61 cm rectangular opening of the observation booth provided relative depth cues in the form of occlusion edges to the observer. There was a distance of approximately 60 cm from the front end of the booth to the screen. The visual angle of the display inside the booth was 90° x 65°. The experimental set-up is represented in Figure 9.

Step 1: Computing the equivalent luminance point for each subject.

All the carriers used in the experiment were mean zero signals which yield an physically isoluminant display only when $n = 0$. At this n value the stimulus contains alternating regions of high and low contrast with identical physical mean luminance at all regions in the display. When non-linearities exist in the transduction process, the transduced signal may not be perceptually isoluminant at $n = 0$ (For example, luminance artifacts may arise from non-linearities in CRT displays or non-linearities may arise within the observer's visual system; Smith & Ledgeway, 1997). In effect, Fourier components may be introduced into motion stimuli when they are assumed to be absent. To compensate for possible nonlinearities due to the transduction process, the point of psychophysical isoluminance was determined for each carrier type for each subject using a method based on the minimum-motion method for measuring the effective luminance of a pattern (Brown, 1995).

Stimuli

Each stimulus sequence consisted of four frames, two low frequency counterphase vertical sine wave gratings interleaved with two counterphase gratings defined by contrast

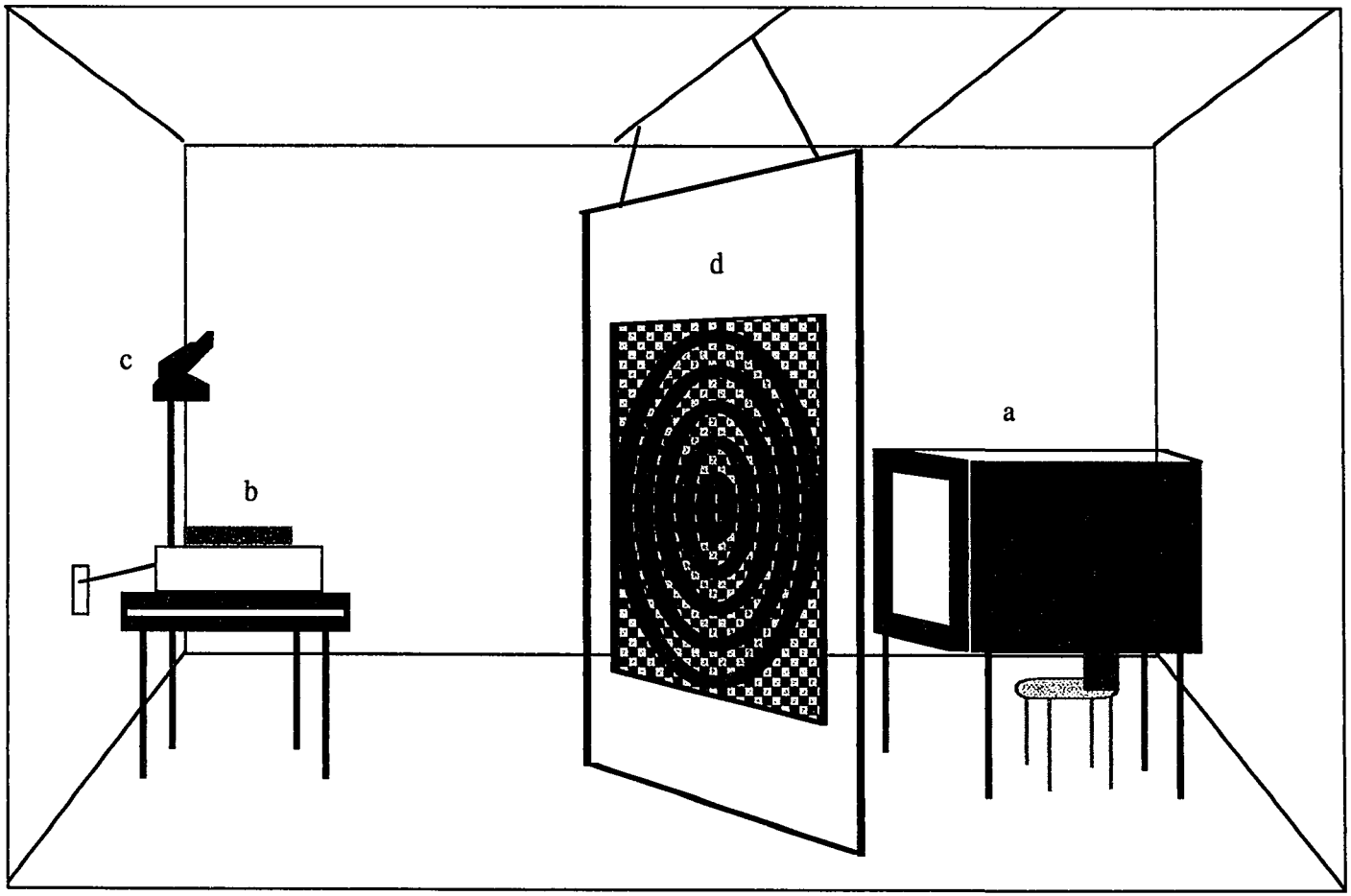

Figure 9. Depiction of the experimental set-up. Subjects viewed the stimuli from inside an observation booth (a). Stimuli were back projected from a projection panel (b) connected to a Dukane overhead projector (c) onto a large screen (d) placed in front of the observation booth.

modulations which were displaced by a quarter cycle from their sine wave counterparts. An example of this sequence is shown in Figure 10. To create stimuli which approximated the nonFourier stimuli used in Step 2, three stimulus sequences were created using different carriers. Two carriers, one vertical and one horizontal, had a spatial frequency three times that of the vertical modulator and the remaining carrier was random noise (Figures 11a, b, and c.)

The low contrast regions of the contrast modulated carrier were fixed in intensity and the high contrast region varied with the *n* value. When the high contrast regions of the contrast modulation were perceptually brighter than the low contrast regions, motion was perceived in a rightward direction because the visual system matches areas of similar brightness on each frame to determine the direction of motion. For similar reasons, motion was perceived in a leftward direction when high contrast regions are perceptually darker than the low contrast regions. At the point where the high and low contrast regions are perceptually isoluminant, the direction of motion of the image was ambiguous to the observer.

Procedure

Interleaved grating sequences were created for each carrier and the isoluminance point of each carrier was determined separately for each. Subjects were presented with 15 second motion sequences as described above and asked to indicate the perceived direction of motion by pressing predetermined computer keys (von Grünau & Dubé, 1993). Subjects were informed that some stimuli would give rise to ambiguous motions while other stimuli would give rise to more stable motion percepts. The method of constant stimuli was used with *n* ranging from -.5 to +.5 in steps of .1 units. A block of randomized trials consisted of one presentation of each of the 11 stimulus conditions. For each carrier type there were two blocks of trials.

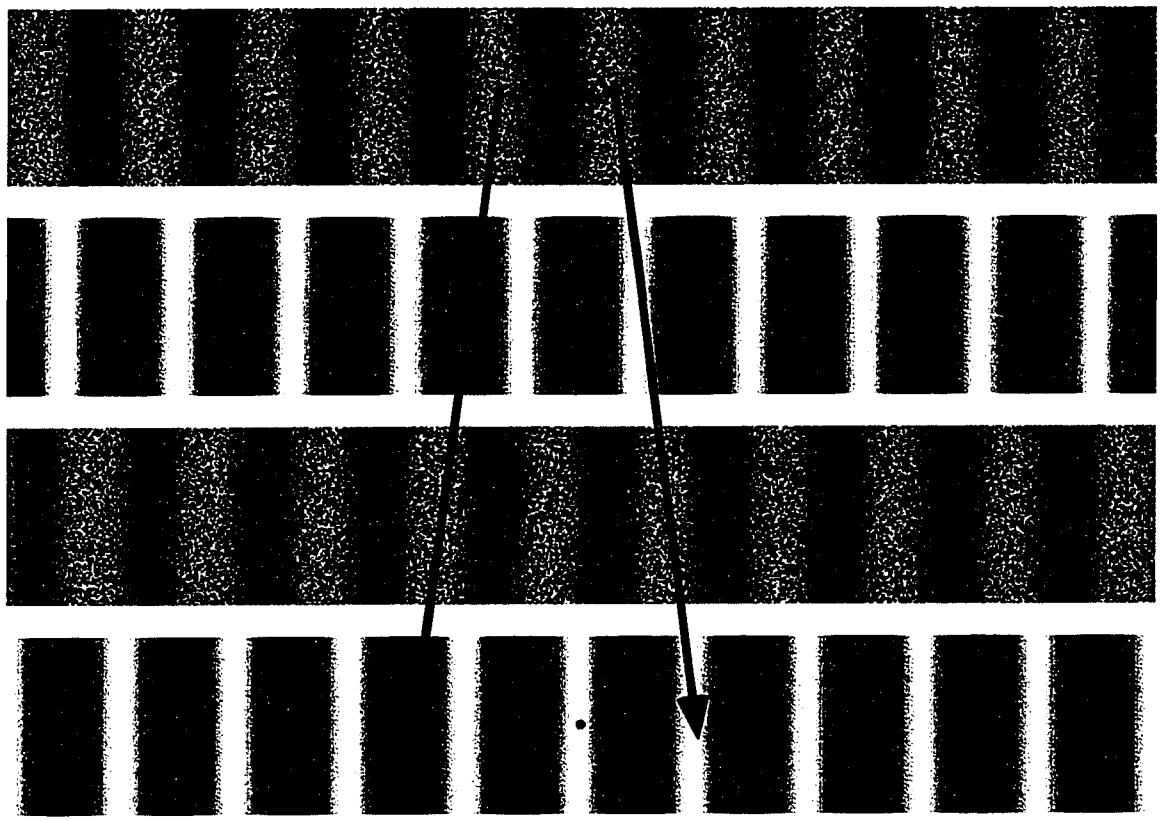

Figure 10. Stimulus sequence used to establish the point of subjective isoluminance. Two counterphase sine wave gratings were interleaved with two counterphase contrast modulated carrier sequences. Each sequence presentation was a quarter cycle out of phase with the sequence presented on the previous frame.

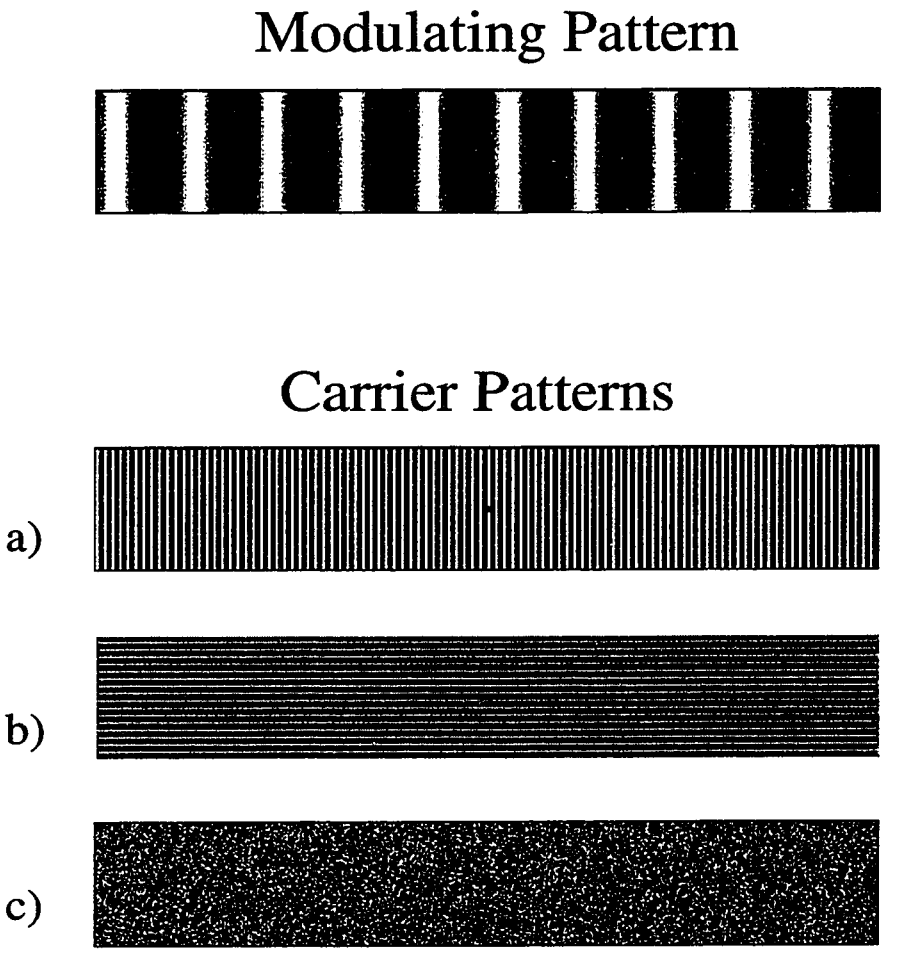

Figure 11. Components of the stimuli used to test psychophysical isoluminance. The modulator (top panel) was combined with one of three static carriers to form the test stimuli described in Figure 6. The concentric carrier (a) has the same form but three times the spatial frequency of the modulator. The radial carrier (b) has the same form as the modulator but has three times the spatial frequency and its spatial orientation is perpendicular to the modulator. The noise carrier (c) is quasi-random noise.

Results

The total time that the test stimulus was seen as moving rightward (R) or leftward (L) was calculated for each observer. The ratio of responses of rightward motion to motion in either direction was computed as R/(R+L). The point at which the resulting function crossed .5 (i.e., the point of equal probability that R or L motion was observed) was deemed to be the psychophysical isoluminance point and will subsequently be designated as $n = 0^*$. Figure 12 shows a typical result for one subject and the isoluminance points for each subject are summarized in Table C1, in Appendix C. Not all the observer's psychophysical isoluminance points corresponded with the point of physical isoluminance ($n = 0$). However, no subject's subjective isoluminance point deviated from the physical isoluminance point by more than .05 units of n. Deviations from the physical isoluminance point occurred in both the positive and negative directions.

Step 2: Testing Vection and Motion Aftereffects.

The question of interest in Experiment 1 was whether the presence or absence of Fourier components in the stimulus has an effect on the inducement of vection and MAE. Therefore only a subset of the nine stimuli described above were required to make this determination.

Six experimental stimuli were formed by the multiplication of V with the three different carriers using two different n values. In one case, n was set to the point of psychophysical luminance for the carrier in question ($n = 0^*$) to eliminate explicit Fourier components in the stimulus. In a second case, n was set to 1 in order to introduce Fourier components into this stimulus. Static representations of the six stimuli are depicted in Figure 11 under the headings $n = 0$ and $n = 1$. The mean luminance in the display was μ

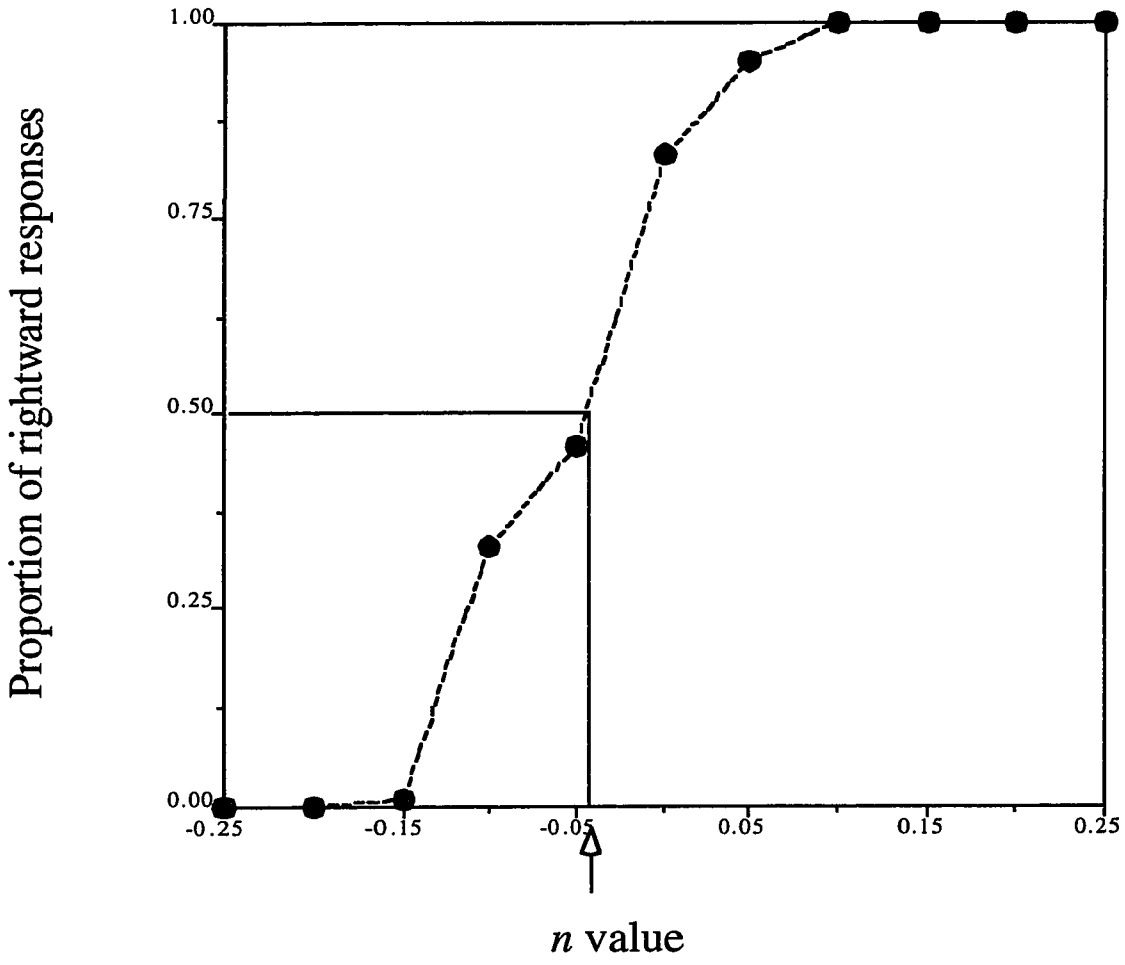

Figure 12. A typical subject's response pattern in the determination of the pscychophysical isoluminance point in Experiment 1. The open arrow on the x-axis indicates the point of pscychophysical isoluminance (n = 0*) for the subject.

when $n = 0$, and $\mu + \alpha$ when $n = 1$. The center of each stimulus was covered by a gray patch to hide aliasing in the highest frequency portions of the stimulus.

Stimuli

The basic vection signal, **V** (Figure 5), was included in the experiment as a control stimulus. The results of the control condition were used as reference to estimate the effectiveness of the experimental stimuli because the control stimulus had previously demonstrated the ability to reliably produce vection and MAE (Potechin, 1995). The control stimulus is simpler than the other stimuli because of the absence of a carrier pattern. It has a background that is consistent with the image flow produced during self-motion.

Procedure

Testing was conducted in a darkened room. Each trial consisted of three parts presented in the following order: 1) a 30 s motion sequence of one of the seven stimuli described above designed to test for vection, 2) presentation of a uniform gray screen for 500 ms, and 3) a 20 s presentation of a static version of the previously moving stimulus to test for MAE. The moving stimulus drifted at 3 Hz, which was determined in pilot studies to be adequate to drive both the vection and MAE illusions in the control conditions. Subjects signaled the presence or absence of each visual illusion by pressing predetermined computer keys. Subjects were asked to press the "/" computer key to indicate the onset of the illusion and no responses were to be made on trials where they did not experience the illusion. Termination of the illusion was signaled by the depression of the "z" computer key. During the vection sequence, subjects could alter their responses as the illusion came and went by switching back and forth between the "/" and "z" keys but during the MAE sequence subjects were asked to record only the onset and offset of the first MAE episode. Each stimulus display was presented six times in random order. Subjects were asked to fixate on a small dot placed slightly below the center of the screen. In many vection

stimulus conditions, the fixation dot was "captured" by the motion in the image and appeared to be moving along the "floor" of the tunnel ahead of the viewer.

Results

Illusion duration and latency to onset (Anderson, 1986; Anderson & Dyre, 1989) were used as the dependent measures. Latency to onset of vection was designated as the time period between the start of the vection stimulus presentation and the subject's initial response (depression of the "/" key). The vection experience could appear intermittently throughout the trial with equal strength and therefore the vection duration measure included multiple vection periods. Vection duration was calculated for each trial as the sum of all time periods between the depression of the "/" and "z" (termination of illusion) keys during the vection stimulus presentation. Latency to onset of MAE was designated as the time period between the start of the test stimulus presentation and the subject's first depression of the "/" key after the appearance of the test stimulus. Only the first MAE episode was considered in the statistical analysis and was calculated as the time period between the depression of the "/" and "z" keys.

The results were analyzed using 4, 3 (carrier) by 2 (*n* value) within subjects, Analyses of Variance (ANOVAs); Latency to onset and Duration for both vection and MAE. The control condition was not included in the statistical analyses. The ANOVA results for Latency to Onset and Duration are summarized in Tables 1 and 2, for both vection and MAE respectively. The means and standard deviations are summarized in Tables A1 and B1, in Appendices A and B, for vection and MAE, respectively. Orthogonal contrasts were also used to determine whether response to the radial carrier differed significantly from that of the other two carriers (Table 3) because the radial carrier

has a representation consistent with veridical image flow produced during forward linear motion through a tunnel while the other two carriers do not. Planned comparisons were used to determine whether the results of the $n = 1$ and the $n = 0^*$ conditions were significantly different for each carrier type (Table 4).

Latency to Onset

MAE

The ANOVA revealed significant results for the main effects of carrier type [$F(2,8) = 12.26$, $p<.01$] and n value [$F(1,4) = 13.44$, $p<.05$] and for the interaction [$F(2,8) = 11.59$, $p<.01$]. As can be seen in the top panel of Figure 13, subjects responded fastest to both types of radial stimuli and slowest to the noise and concentric stimuli where the Fourier components were not explicitly present. The orthogonal contrasts indicated that there was a significant difference between the results of the radial carrier versus the other two carriers for the $n = 0^*$ [$F(1,8) = 40.68$, $p<.001$] but not the $n = 1$ conditions. That is, the performance of the radial carrier versus the other carriers differed for stimuli where the explicit Fourier components were absent but not for stimuli with explicit Fourier components. The planned comparisons indicated that the presence of Fourier components decreased the latency to onset for the concentric [$F(1,8) = 16.62$, $p<.01$] and the noise [$F(1,8) = 41.52$, $p<.001$] carriers but not for the radial carrier.

Vection

The ANOVA revealed significant results only for the main effect of carrier type [$F(2,8) = 8.04$, $p<.05$]. As can be seen in the bottom panel of Figure 13, subjects responded quickest to radial stimuli and approximately equally quickly to noise and concentric stimuli. Although subjects responded more quickly to displays with explicit Fourier components than to the other displays, the difference was not significant. The orthogonal contrasts indicated that there was a significant difference between the results of

Table 1

ANOVAs for latency to onset: Experiment 1

Source	SS	df	MS	F
Motion Aftereffect				
Subject	48.94	4	12.23	
n Value	*158.51*	*1*	*158.51*	*13.44**
n Value x Subject	47.17	4	11.79	
Carrier Type	96.27	2	48.14	12.26**
Carrier Type x Subject	31.42	8	3.93	
n Value x Carrier Type	104.86	2	52.43	11.59**
n Value x Carrier Type x Subject	36.20	8	4.52	
Vection				
Subject	1463.27	4	365.82	
n Value	67.98	1	67.98	3.23
n Value x Subject	84.25	4	21.06	
Carrier Type	887.34	2	443.67	8.04*
Carrier Type x Subject	441.74	8	55.22	
n Value x Carrier Type	1.99	2	1.00	0.13
n Value x Carrier Type x Subject	60.94	8	7.62	

Note. Where appropriate, all degrees of freedom have been adjusted using the Hundt-Felt Epsilon.

*$p < 0.05$. **$p < 0.01$.

Table 2

ANOVAs for duration: Experiment 1

Source	SS	df	MS	F
Motion Aftereffect				
Subject	79.16	4	19.79	
n Value	148.87	1	148.87	135.47***
n Value x Subject	4.40	4	1.10	
Carrier Type	132.25	2	66.13	23.42**
Carrier Type x Subject	22.58	8	2.82	
n Value x Carrier Type	3.86	2	1.93	1.18
n Value x Carrier Type x Subject	13.08	8	1.63	
Vection				
Subject	1636.40	4	409.10	
n Value	92.22	1	92.22	8.53*
n Value x Subject	43.25	4	10.81	
Carrier Type	794.32	2	397.16	13.80**
Carrier Type x Subject	230.20	8	28.78	
n Value x Carrier Type	6.39	2	0.64	0.55
n Value x Carrier Type x Subject	39.77	8	4.97	

Note. Where appropriate, all degrees of freedom have been adjusted using the Hundt-Felt Epsilon.

*$p < 0.05$. **$p < 0.01$. ***$p < 0.001$.

Table 3

Post hoc analyses comparing the radial versus the concentric and noise carriers: Experiment 1

Source	SS	df	MS	F
Latency to Onset of MAE				
n Value = 1	0.00	1	0.00	0.00
n Value = 0	184.09	1	184.09	40.69***
Latency to Onset of Vection				
n Value = 1	419.76	1	419.76	55.10***
n Value = 0	443.86	1	443.86	58.27***
MAE Duration				
n Value = 1	45.55	1	45.55	27.87***
n Value = 0	89.94	1	89.94	55.03***
Vection Duration				
n Value = 1	468.20	1	468.20	94.19***
n Value = 0	331.16	1	331.16	66.62***

Note. Where appropriate, all degrees of freedom have been adjusted using the Hundt-Felt Epsilon.

***$p < 0.001$.

Table 4

Post hoc analyses comparing the FO ($n = 1$) versus the SO ($n = 0$*) carriers: Experiment 1

Source	SS	df	MS	F
Latency to Onset of MAE				
Concentric	75.19	1	75.19	16.62**
Radial	0.33	1	0.33	0.07
Noise	187.85	1	187.85	41.52***
Latency to Onset of Vection				
Concentric	15.79	1	15.79	2.07
Radial	19.58	1	19.58	2.57
Noise	34.60	1	34.60	4.54*
MAE Duration				
Concentric	57.49	1	57.49	35.18***
Radial	29.87	1	29.87	18.28**
Noise	65.36	1	65.36	39.99***
Vection Duration				
Concentric	16.53	1	16.53	3.33
Radial	56.71	1	56.71	11.41**
Noise	25.38	1	25.38	5.11

Note. Where appropriate, all degrees of freedom have been adjusted using the Hundt-Felt Epsilon.

*$p < 0.05$. **$p < 0.01$. ***$p < 0.001$.

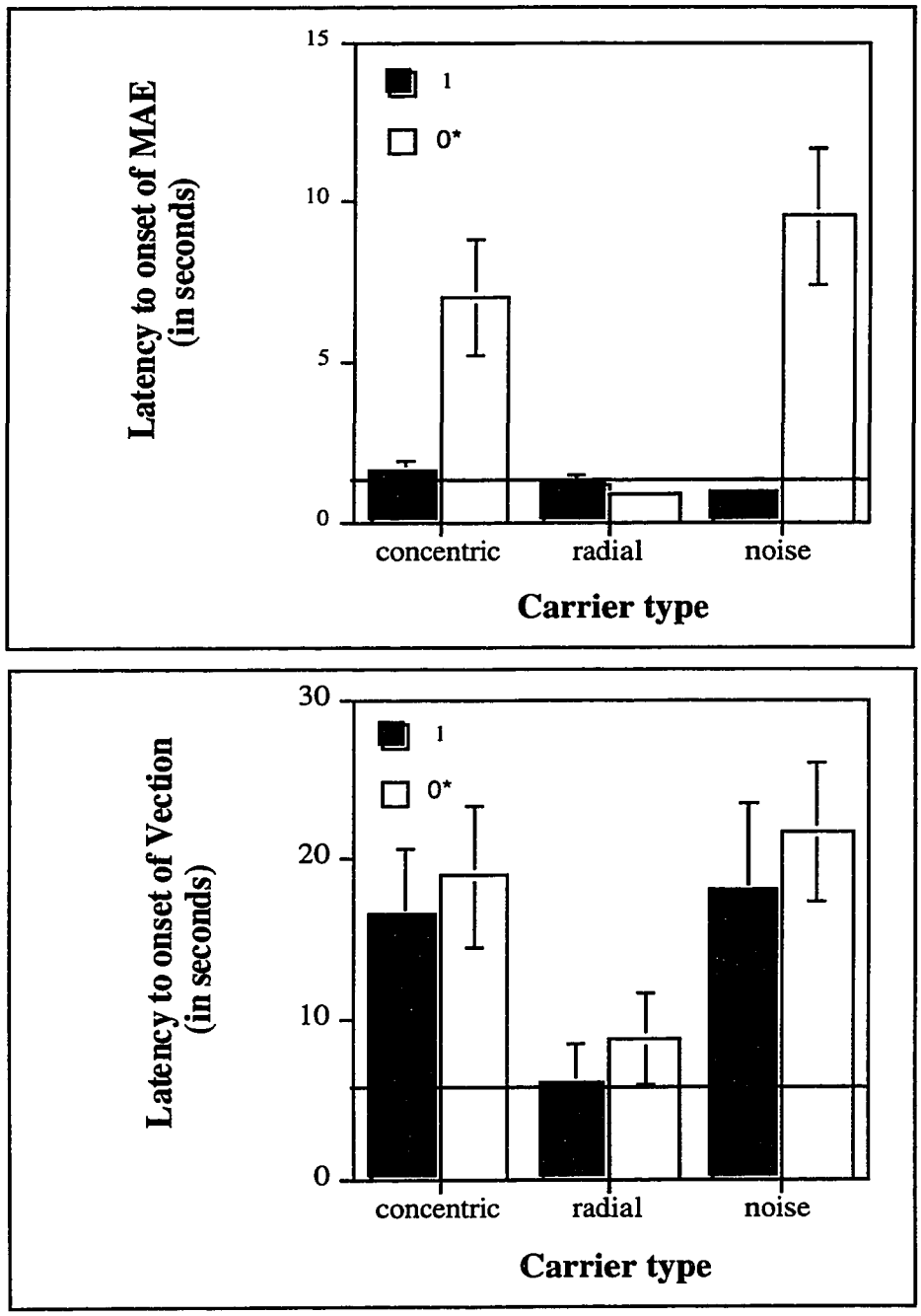

Figure 13. Results of the latency to onset conditions of Experiment 1 plotted as a function of carrier type (concentric, radial, noise) and *n* value(1, 0*). The solid line in both panels is the mean response to the control condition.

the radial carrier versus the other two carriers for both the $n = 0^*$ [$F(1,8) = 55.02$, $p<.001$] and $n = 1$ conditions [$F(1,8) = 27.87$, $p<.001$]. That is, the performance of the radial carrier always differed from that of the other carriers. The planned comparisons indicated that the presence of Fourier components did not affect the latency to onset for any of the carrier types.

Duration

MAE

The ANOVA revealed significant results for the main effects of carrier type [$F(2,8) = 66.13$, $p<.001$] and n value [$F(1,4) = 135.47$, $p<.01$] but not for the interaction. As can be seen in the top panel of Figure 14, the longest responses were elicited by radial carrier stimuli and by stimuli where explicit Fourier components were present. The orthogonal contrasts indicated that there was a significant difference between the results of the radial carrier versus the other two carriers for both the $n = 0^*$ [$F(1,8) = 58.27$, $p<.001$] and $n = 1$ conditions [$F(1,8) = 55.10$, $p<.001$]. Performance of the radial carrier always differed from that of the other carriers. The planned comparisons indicated that the presence of Fourier components increased the duration of MAE for all three carrier types, [$F(1,8) = 35.18$, 39.99 $p<.001$, and 18.28, $p<.01$] for the concentric, noise, and radial carriers, respectively.

Vection

The vection duration results were similar to those of MAE duration. The ANOVA revealed significant results for the main effects of carrier type [$F(2,8) = 13.80$, $p<.01$] and n value [$F(1,4) = 8.53$, $p<.05$] but not for the interaction. Again, the longest responses were elicited by radial carrier stimuli and by stimuli where explicit Fourier components were present, as can be seen in the bottom panel of Figure 14. The orthogonal contrasts indicated that there was a significant difference between the results of the radial carrier

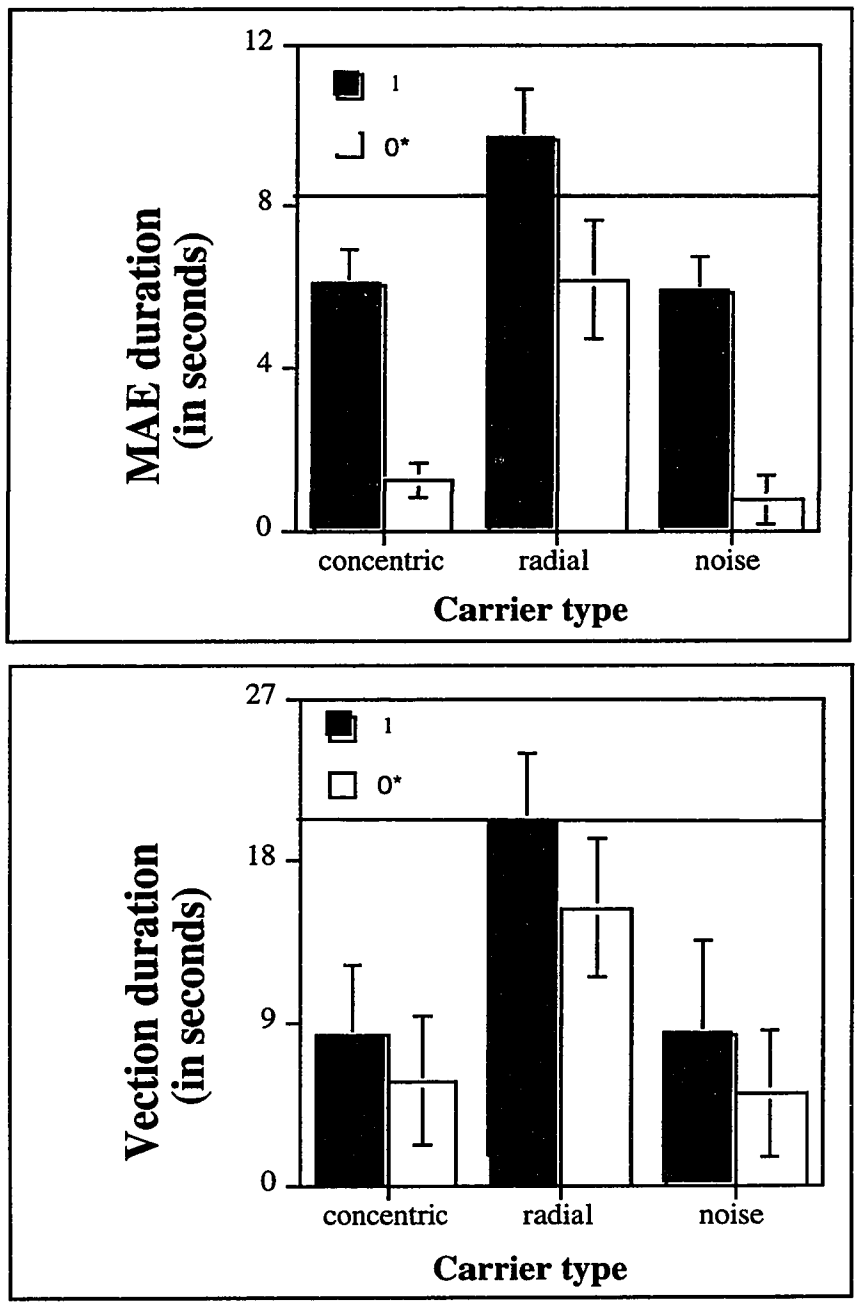

Figure 14. Results of the duration conditions of Experiment 1 plotted as a function of carrier type (concentric, radial, noise) and *n* value(1, 0*). The solid line in both panels is the mean response to the control condition.

versus the other two carriers for both the n = 0* [$F(1,8) = 55.02$, $p<.001$] and n = 1 conditions [$F(1,8) = 27.87$, $p<.001$]. Performance of the radial carrier always differed from that of the other carriers. The planned comparisons indicated that the presence of Fourier components increased the vection duration of the radial stimuli [$F(1,8) = 11.41$, $p<.01$] but not the other carrier types.

The mean data for vection and MAE were highly correlated for illusion duration ($r=.88$) and moderately correlated for latency to illusion onset ($r=.70$) suggesting that the motion mechanisms underlying both illusions may be affected in similar fashion by the visual stimuli used in this experiment. All stimuli were able to induce the two illusions but not to an equal extent. Vection and MAE duration were significantly decreased in response to stimuli where the local Fourier components of **V** were absent. These results support the argument that two mechanisms exist to encode stimuli for the two motion classes, FO and SO motion. The mechanism which encodes FO stimuli will strongly induce the MAE and provides strong inputs into the mechanism responsible for the vection illusion. The mechanism responsible for SO motion encoding induces very poor MAEs although it appears to provide at least moderate input into the vection process.

The Post hoc analyses comparing the FO versus SO stimuli for each carrier type separately indicated that explicit Fourier components in the stimulus had a greater effect in the case of MAE than in the case of vection. There was a significant difference in all the MAE comparisons except in the case of latency to onset for the radial stimulus. On the other hand, only the duration of vection for the radial carrier appeared to be affected by the presence of explicit Fourier components in the stimulus.

The latency to onset results did not demonstrate as clear a pattern as the duration results. In most cases, increased latency to onset occurred in response to stimuli in which local Fourier components of **V** were absent. The one exception was when the radial carrier conditions for MAE did not differ significantly. The radial carrier differed from the other two carriers in all cases which may be related to the fact that this stimulus produces a

motion signal which is consistent with natural self-motion through a tunnel while the other two stimuli do not.

Motion stimuli made up of two components may alternate between periods of transparency and coherence (Adelson & Movshon, 1982; von Grünau & Dubé, 1993). For the stimuli used in this experiment, transparency occurs when the modulator and the carrier are seen as two separate structures originating from different surfaces. For example, the noise stimulus would be seen as a static wall of dots with rings expanding in front of it. Alternatively, the two components may cohere to form a more complex image which appears to move as one unit. In this case, the stimulus is viewed as a tunnel. Most subjects spontaneously reported that 1) vection was achieved in response to motion images which were coherent and 2) that the radial stimulus was easier to see as being coherent. When the display was perceived as being transparent, the static portion of the image, the carrier, was always perceived to be in the background and expanding rings were perceived as making up the foreground. This distinction was not mentioned as being important for the perception of MAE. This point will be discussed further in the general discussion. For the present, the focus remains on the FO versus SO distinction.

EXPERIMENT 2

The results of Experiment 1 suggested that stimuli containing Fourier motion components of **V** produce longer vection durations and longer MAEs than stimuli for which the Fourier components of **V** are absent. An alternative explanation for the obtained results is that the overall luminance of the display rather than the presence or absence of explicit Fourier components is responsible for the differences in vection and MAE durations. In Experiment 1, when n was set to zero, the mean luminance in the display

was approximately equal to μ but when n was set to 1, mean luminance increased to $\mu + \alpha$ (see Equation 5 in the general explanation of the stimuli). Therefore it might be argued that the mean luminance differences in the displays rather than the presence or absence of Fourier components was responsible for the demonstrated differences in Experiment 1.

To rule out the possibility that changes in mean luminance level are responsible for the results obtained in the previous experiment, Experiment 1 was repeated using three n levels (-1, 0*, and 1). The $n = 1$ and $n = -1$ displays both contain the Fourier components of **V** but have higher or lower mean luminances, respectively, than the $n = 0$* displays. For $n = -1$, 0, and 1, the Michelson contrasts are .82, .45, and .31 respectively. If contrast is defined in terms of the expected mean intensities in the peaks and troughs of the contrast modulations then the contrasts for n = -1, 0, and 1 are .29, 0.0, and .18, respectively. These contrasts show a quadratic dependence on n with a minimum at $n = 0$ because the mean luminance is the same in the peaks and troughs of the contrast modulation. If MAEs and vection are influenced by the overall luminance level of the display then one would expect there to be a linear relationship between n value and illusion strength. Conversely, if MAE and vection are dependent on the presence of Fourier components in the display, then illusion strength should be at it's lowest when $n = 0$*.

Method

Subjects

Six subjects (2 males, 4 females) participated in both steps of the experiment. Two of the subjects had participated in Experiment 1 and the rest were naive observers. All reported 20/20 or corrected to 20/20 vision

Procedure

The procedure for steps 1 and 2 for Experiment 2 was identical to that of Experiment 1 with the following exceptions:

Step 1: Computing the equivalent luminance point for each subject

The equivalent luminance point for each subject was computed using the identical procedure to that used in Experiment 1. The isoluminance points for each subject are summarized in Table C1. As in Experiment 1, no subject's psychophysical isoluminance point deviated from the physical isoluminance point by more than .05 units. For all subjects, the psychophysical isoluminance point was almost always equal to or slightly below the point of physical isoluminance. The one exception occurred for subject 5 in the radial condition.

Step 2: Testing Vection and Motion Aftereffects.

Stimuli

Ten different stimulus displays were used in the experiment. The control stimulus was the basic vection signal, V, shown in Figure 5. Nine experimental stimuli were formed by the multiplication of V with the three different carriers used in Experiment 1 (Figures 6a,b,c), with the parameter n set to three different values (see Equation 6). In one case, n was set to the point of psychophysical isoluminance for the carrier in question (n = 0*) to eliminate explicit Fourier components of **V** in the stimulus. Otherwise, n was set to either +1 or -1 to introduce Fourier components into the stimulus. In effect, three additional stimulus displays were tested in addition to those used in Experiment 1. Figure

11 depicts static versions of the stimulus set used in this experiment, which was described at the end of the introduction.

Results

Illusion duration and latency to onset were used as the dependent measures and were calculated as described in Experiment 1. The results were analyzed using 4, 3 (carrier) by 2 (*n* value) within subjects, Analyses of Variance (ANOVAs); Latency to onset and Duration for both vection and MAE. The control condition was not included in the statistical analyses. The ANOVA results for Latency to Onset and Duration are summarized in Tables 5 and 6, for both vection and MAE respectively. The means and standard deviations are summarized in Tables A2 and B2, for both vection and MAE respectively. Quadratic trends (as a function of *n* value) were tested separately for each carrier and are summarized in Table 7. Orthogonal contrasts were also used to determine whether the results of the n = 1 and the n = -1 conditions differed for each carrier type and are summarized in Table 8.

Latency to Onset

MAE

The ANOVA revealed a significant main effect of *n* value [$F(2.10) = 4.78$, $p<.05$]. The main effect of carrier type and the interaction were not significant. As can be seen in the top panel of Figure 15, the shortest onset intervals were elicited by stimuli where the Fourier components of **V** were not explicitly present. The quadratic trend (as a function of *n* value) was significant for the noise carrier [$F(1,20) = 24.39$, $p<.001$] but not for the other two carriers. The orthogonal contrasts indicated that there were no significant differences between the results for the $n = -1$ and the $n = 1$ conditions for any of the carriers. That is, there was no difference between subject performance in response to

Table 5

ANOVAs for latency to onset: Experiment 2

Source	SS	df	MS	F
Motion Aftereffect				
Subject	886.81	5	177.36	
n Value	186.11	2	93.06	4.78*
n Value x Subject	194.67	10	19.47	
Carrier Type	52.18	2	26.09	3.73
Carrier Type x Subject	69.96	10	7.00	
n Value x Carrier Type	69.72	4	17.43	2.02
n Value x Carrier Type x Subject	172.134	20	8.61	
Vection				
Subject	1316.85	5	263.37	
n Value	139.56	2	69.78	7.92**
n Value x Subject	88.14	10	8.81	
Carrier Type	368.80	2	184.4	2.82
Carrier Type x Subject	654.78	10	65.48	
n Value x Carrier Type	17.49	4	4.37	0.50
n Value x Carrier Type x Subject	175.29	20	8.76	

Note. Where appropriate, all degrees of freedom have been adjusted using the Hundt-Felt Epsilon.

*$p < 0.05$. **$p < 0.01$.

Table 6

ANOVAs for duration: Experiment 2

Source	SS	df	MS	F
Motion Aftereffect				
Subject	98.58	5	19.72	
n Value	240.14	2	120.07	10.64**
n Value x Subject	112.90	10	11.29	
Carrier Type	214.75	2	107.37	28.12***
Carrier Type x Subject	38.18	10	3.82	
n Value x Carrier Type	10.72	4	2.68	1.58
n Value x Carrier Type x Subject	33.81	20	1.69	
Vection				
Subject	1677.02	5	335.40	
n Value	263.99	2	132.00	14.37**
n Value x Subject	91.85	10	9.18	
Carrier Type	874.75	2	437.37	4.12*
Carrier Type x Subject	1060.60	10	106.06	
n Value x Carrier Type	40.64	4	10.16	0.75
n Value x Carrier Type x Subject	272.33	20	13.62	

Note. Where appropriate, all degrees of freedom have been adjusted using the Hundt-Felt Epsilon.

*$p < 0.05$. **$p < 0.01$. ***$p < 0.001$.

Table 7

Post hoc analyses comparing the FO (n = 1 or -1) versus the SO (n = 0*) carriers: Experiment 2

Source	SS	df	MS	F
Latency to Onset of MAE				
Concentric	31.14	1	31.14	3.62
Radial	11.19	1	11.19	1.30
Noise	209.90	1	209.90	24.39***
Latency to Onset of Vection				
Concentric	60.93	1	60.93	6.95*
Radial	18.48	1	18.48	2.11
Noise	65.86	1	65.86	7.51*
MAE Duration				
Concentric	34.99	1	34.99	20.70***
Radial	94.89	1	94.89	56.13***
Noise	90.64	1	90.64	53.62***
Vection Duration				
Concentric	134.09	1	134.09	9.85**
Radial	24.03	1	24.03	1.76
Noise	135.89	1	135.89	9.98**

Note. Where appropriate, all degrees of freedom have been adjusted using the Hundt-Felt Epsilon.

*** $p < 0.001$ ** $p < 0.01$ * $p < 0.05$

Table 8

Post hoc analyses comparing high (n = 1) versus low (n = -1) luminance displays for each carrier: Experiment 2

Source	SS	df	MS	F
Latency to Onset of MAE				
Concentric	1.41	1	1.41	.16
Radial	0.47	1	0.47	.82
Noise	1.73	1	1.73	.20
Latency to Onset of Vection				
Concentric	9.28	1	9.28	1.06
Radial	1.15	1	1.15	.13
Noise	1.35	1	1.35	.15
MAE Duration				
Concentric	7.84	1	7.84	4.64*
Radial	16.60	1	16.60	9.82**
Noise	5.90	1	5.90	3.49
Vection Duration				
Concentric	5.19	1	5.19	.38
Radial	0.19	1	0.19	.01
Noise	5.24	1	5.24	.38

Note. Where appropriate, all degrees of freedom have been adjusted using the Hundt-Felt Epsilon.

** $p < 0.01$ * $p < 0.05$

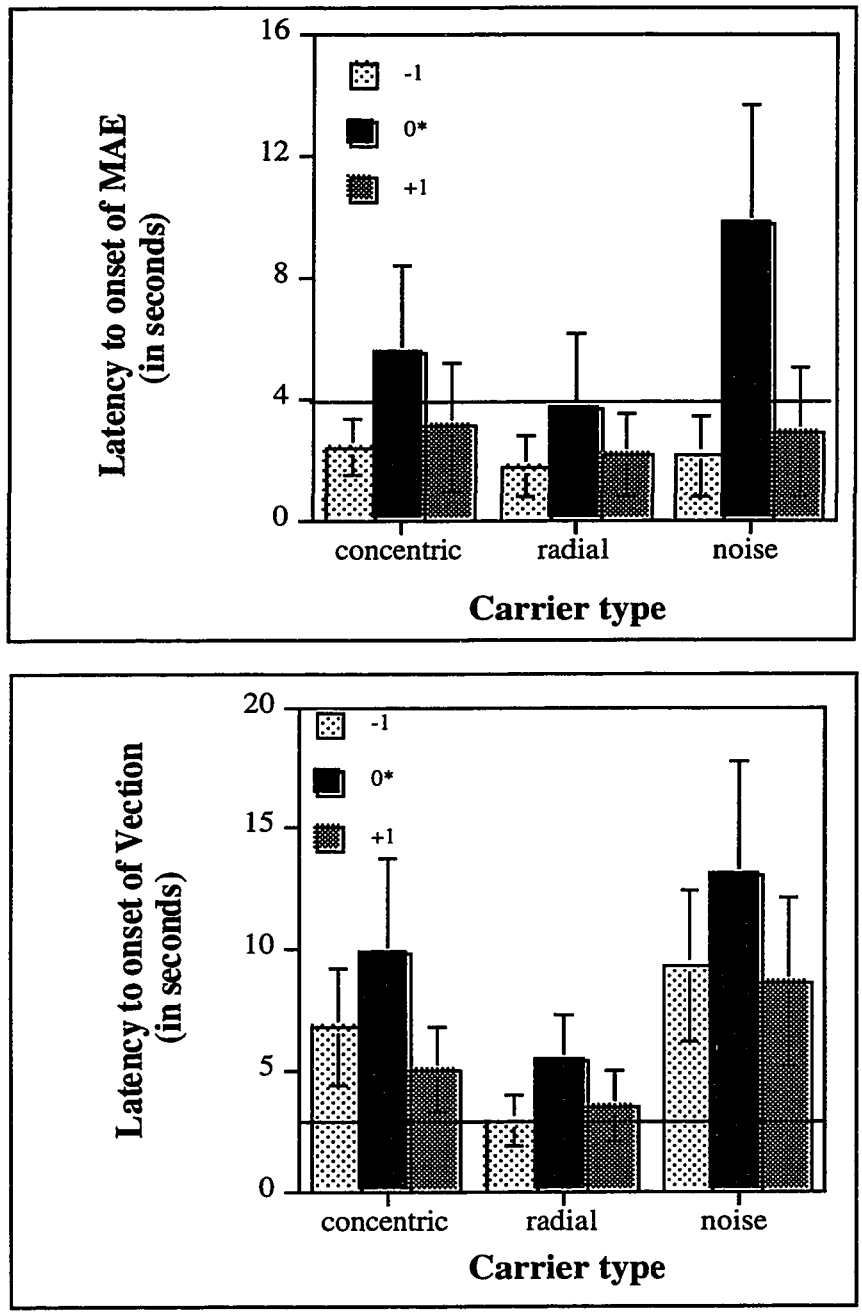

Figure 15. Results of the latency to onset conditions of Experiment 2 plotted as a function of carrier type (concentric, radial, noise) and *n* value(-1, 0*, and 1). The solid line in both panels represents the mean response to the control condition.

stimulus types with explicit Fourier components but with different overall luminance levels in the display.

Vection

The ANOVA revealed a significant main effect of *n* value [$F(2,10) = 7.92$, $p<.01$] and a marginal trend of carrier type [$F(2,10) = 2.82$, $p<.11$]. The interaction was not significant. As can be seen in the bottom panel of Figure 15, the onset of vection took longer in response to stimuli where the explicit Fourier components of **V** were absent. The quadratic trend (as a function of *n* value) was significant for the concentric carrier [$F(1,20) = 6.95$, $p<.05$] but not for the other two carriers. The orthogonal contrasts indicated no significant differences between the $n = -1$ and the $n = 1$ conditions for any of the carriers.

Duration

MAE

The ANOVA revealed significant main effects of carrier type [$F(2,10) = 28.12$, $p<.01$] and *n* value [$F(2,10) = 10.64$, $p<.01$]. The interaction was not significant. As can be seen in the top panel of Figure 16, radial stimuli and stimuli with explicit Fourier components produced longer MAE durations. The quadratic trend (as a function of *n* value) was significant for all three carriers [$F(1,20) = 20.696$, 56.13, and 53.61, $p<.001$ for the concentric, radial, and noise carriers, respectively]. The orthogonal contrasts indicated that there were significant differences between the results for the $n = -1$ and the $n = 1$ conditions for the concentric [$F(1,20) = 4.64$, $p<.05$] and radial carriers [$F(1,20)$ 9.82, $p<.01$] but not for the noise carrier.

Vection

The vection duration results were similar to the MAE durations. The ANOVA revealed significant results for the main effects of carrier type [$F(2,10) = 4.12$, $p<.05$] and

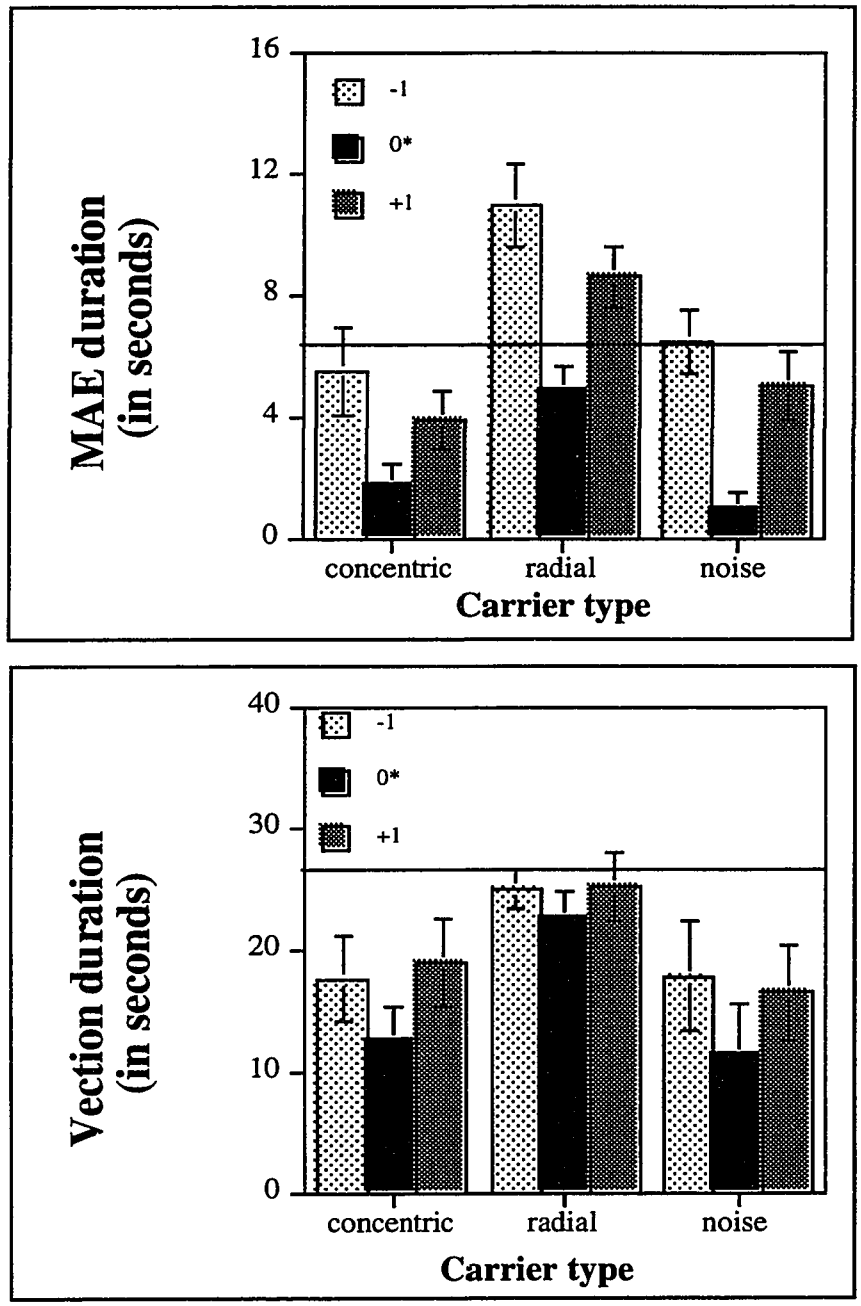

Figure 16. Results of the duration conditions of Experiment 2 plotted as a function of carrier type (concentric, radial, noise) and *n* value(-1, 0*, and 1). The solid line in both panels is the mean response to the control condition.

n value [F(2,10) 14.37, p<.15] but not for the interaction. Again, the longest responses were elicited by radial carrier stimuli and by stimuli where explicit Fourier components were present, as can be seen in the bottom panel of Figure 16. The quadratic trend (as a function of *n* value) was significant for the concentric [F(1,20) = 9.85, p<.01] and noise carriers [F(1,20) = 9.98, p<.01] but not for the radial carriers. The orthogonal contrasts indicated no significant differences between the $n = -1$ and the $n = 1$ conditions for any of the carriers.

Had mean luminance levels been related to vection and MAE, illusion strength should have been strongest in the $n = 1$ conditions, followed by the $n = 0^*$ conditions, and weakest in the $n = -1$ conditions but this was not the case. In fact, illusion strength was at its lowest level in the $n = 0^*$ conditions and was not significantly different in the $n = 1$ and $n = -1$ conditions for all three carriers. Therefore, the results suggest that vection and MAE strength are not dependent upon overall luminance levels in the displays.

For both vection and MAE, illusion strength was decreased (in terms of duration and latency to onset) when local first-order components of **V** were absent from the stimulus. Again, the mean data for vection and MAE were highly correlated for illusion duration (r=.82) and moderately correlated for latency to illusion onset (r=.69) suggesting that the vection and MAE were affected similarly by the independent variables.

EXPERIMENT 3

Smith and Ledgeway (1997) criticized the use of contrast modulated static carriers to examine the FO versus SO distinction. In particular, they examined contrast modulated noise, which is commonly used to create SO motions. Smith and Ledgeway argued that whenever there is an imbalance in the ratio of light to dark pixels in a local region of the carrier the drifting contrast modulation would produce drifting luminance modulations that

are detectable by a standard (FO) motion energy mechanism. Increasing the size of the individual noise units within a given area serves to increase the probability of contamination by luminance artifacts. Smith and Ledgeway concluded that detection of "SO motion" stimuli may actually reflect the detection of FO artifacts. If their conclusion is correct, many motion experiments comparing FO and SO effects may actually have compared two types of FO motions.

Using static and dynamic noise patterns, Benton and Johnston (1997) verified that the application of a standard energy model to contrast modulated noise stimuli will result in clearly detected motion in local patches of the stimulus. Furthermore, by increasing noise element size and/or decreasing noise dimensionality from dynamic to static increases the probability of contamination of the SO image by luminance artifacts. However, the motion detected in local patches of the contrast modulations does not occur in the same direction at each location. Benton and Johnston (1997) concluded that perception of SO motion in a constant direction cannot be explained by a direct process of ME extraction because there is a high probability that the luminance artifacts will be directionally balanced in contrast modulated stimuli.

Gurnsey, Fleet, and Potechin (1998) came to a different conclusion based on their ME analysis of contrast modulated noise stimuli. Initially, they used linearly translating stimuli with noise element sizes ranging from 1 to 128 pixels. To estimate the response of both FO and SO motion mechanisms, a ME mechanism was applied to both the raw image luminance intensities (FO channel) and to a signal convolved with a small center-surround filter before being half-wave rectified (approximation of a SO channel). The results of this analysis indicated that local FO energy increased while SO energy decreased as a function of noise element size.

A further analysis by Gurnsey et al. (1998) compared the two ME mechanisms' responses to the linearly translating stimuli identical to the SO noise stimuli used in Experiments 1 and 2 for the $n = 0$ and $n = 1$ conditions. The results of this comparison

indicated that ME responses for SO mechanisms were virtually the same in the $n = 0$ and $n = 1$ conditions. However, the response of the FO mechanism showed a greatly reduced response when $n = 0$. This may explain the reduced illusion strength noted in the previous experiments for the $n = 0^*$ conditions.

Based on the ME model analysis by Gurnsey et al. (1998) , one could question whether the responses to SO stimuli reported in Experiments 1 and 2 were actually the result of the workings of a SO channel because the results can be explained by way of referring exclusively to the operation of a FO channel. The assertion that only one motion channel is required to support FO and SO motion perception is consistent with this argument. Conversely, one could argue that a basic difference in the FO and SO stimuli was responsible for the results obtained rather than the motion system engaged. To address this question, Experiment 3 was conducted to determine how MAE and vection are affected by an increase in the probability of local luminance artifacts in contrast modulated noise stimuli.

Method

Subjects

All six subjects (2 males, 4 females) who participated in Experiment 3 had participated in Experiment 2. All subjects reported 20/20 or corrected to 20/20 vision.

Stimuli

Nine different stimulus displays were used in the experiment. The control stimulus was the basic vection signal, V, shown in Figure 5. Eight experimental stimuli were formed by the multiplication of V with static noise carriers having different check sizes. The check widths were determined as follows:

$$\text{Check width} = 2^m$$

Where m was a value in the range of 0 to 7. Examples of the stimuli used in the experiment can be seen in Figure 17. As the pixel size is increased, there is an increased probability that local motions within the stimulus will be luminance defined rather than contrast defined.

Procedure

The procedure for Experiment 3 was identical to that of Experiment 1 except that the isoluminance point was not calculated for the eight different check sizes for a couple of reasons. First, the magnitude of a global distortion product which will result from a luminance non-linearity of a given magnitude is not affected by variation in noise pixel size (Smith and Ledgeway, 1997). Second, Smith and Ledgeway (1997) demonstrated that global distortion products had little effect on the pattern of results they obtained when they manipulated the check size in their contrast modulation displays. This indicates that the results obtained using the physical isoluminance point versus the subjective isoluminance point should be the same.

Results

Average duration as a function of check size was used as the dependent measure and was calculated in a similar manner to the duration measures used in Experiments 1 and 2. Latency to onset was not used as a dependent measure because this measure proved to have less reliable results in the first two experiments than the duration measure. The control condition was not included in the statistical analyses. The data were analyzed using 2, one factor (check size) within subjects, ANOVAs; duration for both vection and MAE.

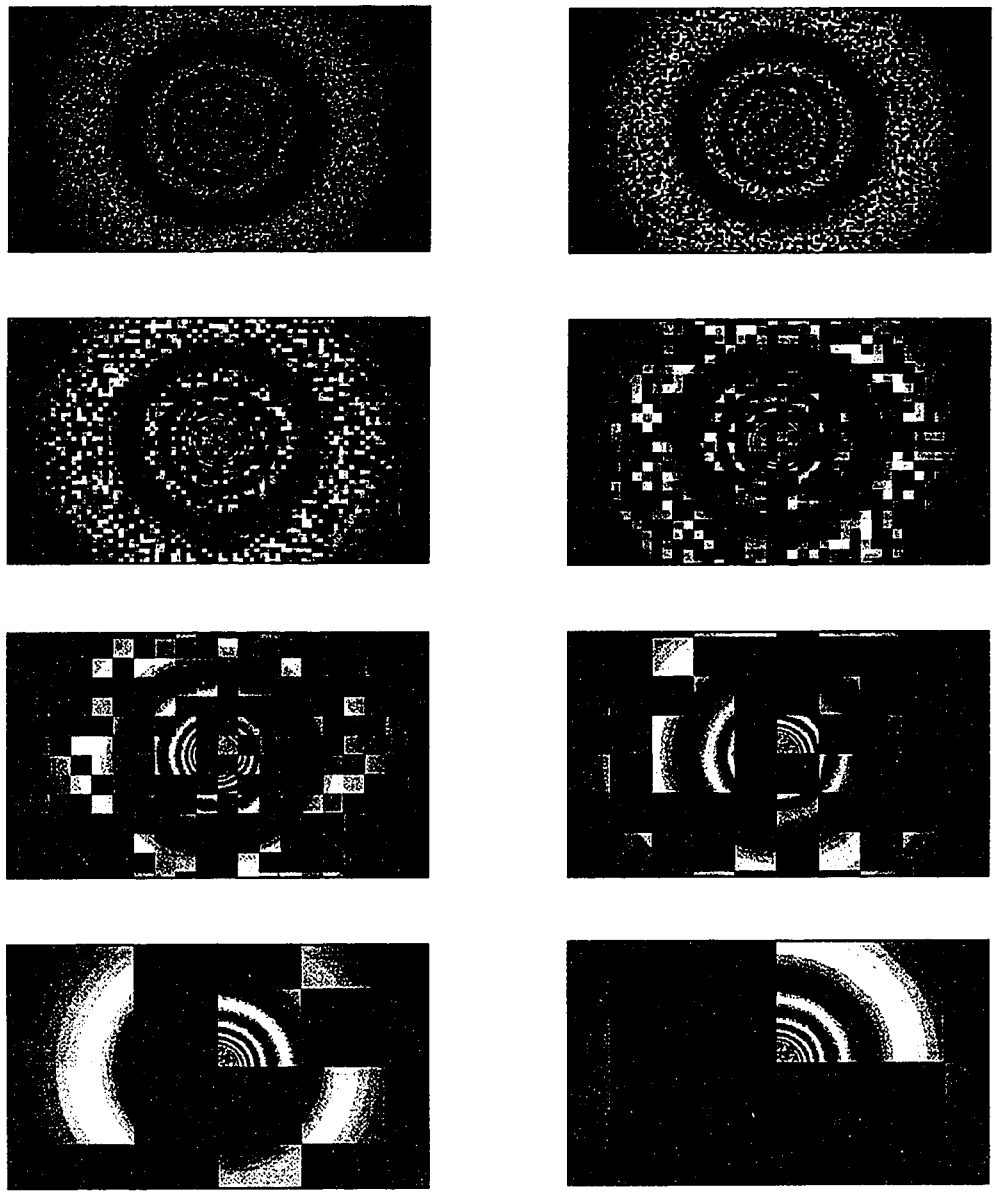

Figure 17. The stimuli used in Experiment 3 arranged in order of increasing check size.

The ANOVA results are summarized in Table 9.

In the case of MAE, the ANOVA revealed a significant effect of check size [$F(7,35) = 10.86$, $p < .001$]. A Tukey-T post-hoc test (Table 10) showed that the responses to stimuli with check sizes of 1 and 2 pixels were significantly different from the responses to all other stimuli at the .01 alpha level except for each other and the display with a check size of 4 pixels. The MAE results are consistent with the argument of Smith and Ledgeway (1997) that SO effects can be explained by the operation of a FO channel in response to FO contamination in the stimulus. That is, if ME increases with check size, MAE duration will also increase with increasing check size, as can be seen in Figure 18. For the case of vection, the ANOVA showed no significant effect of check size. This result suggests that FO contamination in the stimulus is not sufficient to explain SO vection effects in Experiments 1 and 2.

As in Experiment 1, most of the subjects reported that the modulated stimuli gave rise to two percepts, either an integrated image in motion or an image consisting of two parts, of which only one part was in motion. In most conditions, the carrier was perceived as the static portion of the image but for the largest check size displays the carrier could be perceived as either being in the foreground or in the background.

Table 9

ANOVAs for duration: Experiment 3

Source	SS	df	MS	F
Motion Aftereffect				
Subject	376.19	5	75.24	
Check Size	379.77	7	54.25	10.86***
Check Size x Subject	174.83	35	5.00	
Vection				
Subject	86.79	5	17.36	
Check Size	84.32	7	12.04	1.53
Check Size x Subject	276.11	35	7.89	

Note. Where appropriate, all degrees of freedom have been adjusted using the Hundt-Felt Epsilon.

*** $p < 0.001$.

Table 10

Tukey-T Test as a function of stimulus check size (in pixels) for MAE duration: Experiment 3

	2	**1**	**4**	**8**	**16**	**32**	**128**	**64**
2	X	-	-	s	s	s	s	s
1	-	X	-	s	s	s	s	s
4	-	-	X	-	-	-	s	s
8	s	s	-	X	-	-	-	-
16	s	s	-	-	X	-	-	-
32	s	s	-	-	-	X	-	-
128	s	s	-	-	-	-	X	-
64	s	s	s	-	-	-	-	X

Note. $\alpha = .05$ and .01 for the results in the upper and lower triangles, respectively

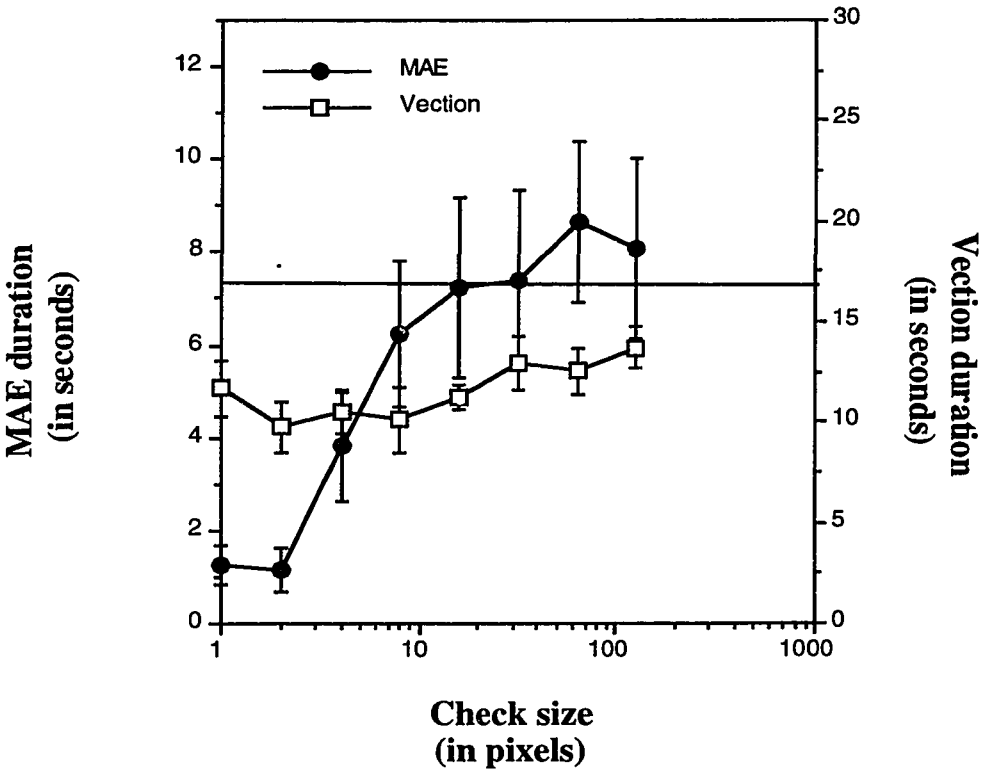

Figure 18. Duration results for Experiment 3. The left and right axes relate to MAE and vection respectively. The axes have been scaled to match the performance of the control condition (solid horizontal bar). MAE durations (black circles) increased along with check size and the highest MAE durations were near the level of the control stimulus. Vection durations (unfilled squares) were relatively unaffected by check size and were always below the level of the control stimulus.

Discussion

Researchers often dichotomize the phenomena they study. For example, short-range versus long-range motion, first-order versus second-order, and Fourier versus non-Fourier motion. While the use of dichotomous classification can simplify the research process, there is a danger that the two categories will be seen as being fundamentally different when they are not different in all cases. FO and SO motions have been shown to differ in their ability to induce motion illusions, such as MAEs and the KDE, in some but not in all cases. In this research project, the FO versus SO dichotomy was studied in three ways: 1) a determination of the relative ability of FO and SO motions to induce vection, 2) a comparison of the relative efficiency of FO and SO motions to induce MAE and vection, and 3) an examination of how MAE and vection were affected by a systematic increase in FO motion components to a SO stimulus. Of particular interest was the determination of whether SO motions can support vection, an illusion which requires computations related to motion in depth.

In the first two experiments, the results appeared to represent the effects of an independent variable which was dichotomous. The stimuli that contained explicit Fourier components produced vection and MAEs of a higher magnitude, in terms of initial reaction time and duration of the illusion, than stimuli in which the Fourier components were greatly minimized. Additionally, the independent variable had relatively similar effects on the two illusions, suggesting that either both vection and MAE processes are either mediated by one motion mechanism or, if two motion mechanisms are required to produce the two illusions, the manipulations of the independent variables affected the two mechanisms in a similar manner. Reduced illusion magnitudes in response to the SO displays could not be attributed to general display luminance levels because the SO stimuli were less effective at eliciting the illusions than FO displays having both higher and lower luminance levels.

In Experiment 3, MAE strength was positively related to the ME in the image, which is consistent with the previous experiments, but vection strength was virtually unaffected by the magnitude of local ME in the image. This difference makes it unlikely that MAE and vection are mediated by a common motion process in the visual system. MAE appears to be driven by a low level visual process because it is a behavior which can be predicted by the activity of low level receptors in the visual system. As vection cannot be predicted on this basis, vection may be driven by a higher level operation such as a process based on feature matching. Johansson (1977) described vection as an all-or-none process. Once the vection experience is initiated, the illusion appears to be perpetuated without regard to the initial evoking stimulus.

Although all stimulus displays drove the vection and MAE illusions to some extent, SO motions produced weaker responses and it is questionable as to whether SO motions can in fact elicit the MAE to any extent. Savoy (1987) noted the virtual impossibility of eliminating all FO signals in an image. Just squinting or changing viewing distance can reintroduce them (Brown, 1995). It can be argued that due to the presence of distortion products the stimuli described in Experiments 1 and 2 as SO had enough motion energy to activate a FO system. Effectively, this would indicate that the experiments reported here did not compare the two stimulus classes intended, namely FO and SO motions, but rather made comparisons between different types of FO stimuli.

However, even if distortion products do exist in SO images, it does not necessarily follow that SO motion is detected on the basis of distortion products. A similar case in point is the role of distortion products in the detection of displacements of spatial beats. Badcock and Derrington (1989) acknowledge that distortion products could exist in spatial beats. However, they argued that beat displacements could not be detected through the use of distortion products because direction discrimination thresholds for spatial beats were not affected when the distortion products were removal through the addition of a nulling grating.

MAE was highly affected by the amount of FO motion energy in the stimuli and it seems reasonable to assume that the small amount of MAE reported in response to SO stimuli could have been due to FO artifacts within the image. As vection was not highly affected by local luminance patches in the display, the moderate vection effects reported in response to SO stimuli may represent the workings of a different mechanism, perhaps a mechanism specialized to detect SO motion.

Smith and Ledgeway (1997) promoted contrast modulated dynamic noise with the smallest noise elements possible as the optimal second-order stimulus. While using dynamic noise rather than static noise to create the SO image may help to eliminate distortion products from the display it may also serve to introduce a new extraneous variable into the experiment, difficulty level of stimulus perception. Dynamic noise displays may increase the internal noise level (Verstraten et al., 1995). That is, due to random stimulation in the visual receptors, the SO motion signal may be masked. Derrington et al. (1993) demonstrated a reduced ability to detect the direction of beat stimuli versus plaid stimuli of comparable spatial structure. The dynamic displays used by Smith and Ledgeway (1997) may seem to cancel out any FO effects because the stimulus was less visible and not because the dynamic display have a reduced amount of motion energy. Therefore, the use of dynamic displays to isolate SO components of the image may not be an improvement over the use of static displays.

The effects of transparency may serve to partially explain why vection strength was independent of noise element size in Experiment 3. The visual system may have only processed the portion of the image which appeared to be in motion, the modulation, and ignored the static image component, the carrier. This would explain why the carrier did not interfere significantly with vection perception even at the largest noise element sizes which constitute a strong signal to the observer that self-motion is not occurring. Based on the results of Experiments 1 and 2, where carrier type was shown to strongly influence vection

strength, it does not appear likely that vection strength is based only on the influence of the modulator.

Transparency may also partially explain the vection results in Experiments 1 and 2 if one considers how the different carrier types would have brought about different levels of transparency between images with different carrier types. Whether an image is perceived as transparent or coherent partially depends on the image luminance properties at the junction of the two components. Images which are incompatible with physical transparency are less likely to be perceived as arising from component motion (Stoner, Albright, & Ramachandran, 1990). The concentric and noise stimuli contained information which was incompatible with physical translation within a tunnel because the luminance pattern changed continuously at the junction of the modulator and the carrier. Additionally, the luminance patterns of the noise and concentric stimuli did not change in size over time as expected when the image flow represents physical objects in the environment which start out at a reasonable distance from the observer. Constant luminance levels at the junction of the two components of the radial stimulus are consistent with the image flow produced while moving through a tunnel and may allow the observer to perceive the radial stimulus as a coherent image.

The vection results may have represented a trade-off between two opposing elements within the stimulus. For example, Brandt et al. (1975) demonstrated that for motion displays made up of two components presented at different depths, circular vection strength was decreased when the background component was a stationary image. In other words, one component of the stimulus is concordant with the image flow during self-motion while one is not. In Experiment 3, as noise unit size increases the visual signal becomes less representative of the optic flow encountered during self-motion if the carrier is perceived to be in the background. This is because stationary backgrounds indicate to the observer that they are not in motion. Observers seem to be able to interpret the noise units as being in motion if noise unit size is small but this becomes less possible as the unit

size increases. One would expect this effect to reduce vection strength but it may be offset by the influence of increasing ME in the stimulus. When the stimulus components were not in opposition, such as in the case of the radial stimuli where the entire display was consistent with visual flow during self-motion, the illusion strength was greatly enhanced in comparison. It is interesting to note vection strength was not greatly affected when the noise units were perceived to be in the foreground, another example of when the stimulus components were not in opposition.

An alternative explanation is that the invariant vection strength represents a combination of effects. Wilson et al. (1992) promoted a motion mechanism in which the outputs of the Fourier and nonFourier pathways are combined to produce a single motion percept and it may be plausible that the vection results represent the combined outputs of FO and SO mechanisms. FO energy increases while SO energy decreases as a function of noise element size in contrast modulated noise patterns (Gurnsey et al., 1998). As the noise unit sizes increase in contrast modulated patterns, the FO and SO vection effects appear in a reciprocal relationship. If the FO and SO inputs were equally balanced in terms of capacity to evoke vection, one might expect that vection strength would be independent of check size in the noise stimulus. As there was a small but insignificant decrease in vection strength as noise element size increased, the contribution of FO energy in this process may be stronger under the right circumstances.

This assumption that FO and SO motions make up the combined inputs to one motion process can also be used to explain the results obtained in Experiments 1 and 2. When $n = 0^*$ only the responses of the SO mechanism provides input to the motion process but when $|n| > 0$ then both FO and SO mechanisms may be at work. Consequently, the differences noted in responses to stimuli of different n values may reflect the amount of input provided by the combined FO and SO mechanisms rather than the type of input being analyzed.

These results differ from those of Dosher et al. (1989) who found that SO stimuli were unable to support the recovery of 3-D structure from 2-D motions. This may be partly explained by the nature of the task and the complexity of the stimuli used in the two studies. Firstly, the KDE uses relative motion cues to evoke the image of an object, outside the observer, rotating in space while converging lines and perspective cues were used to elicit illusory self-motion. That is, the depth cues used by the observer and the viewpoint of the object in motion differs for the two tasks. Secondly, Dosher et al. used an objective task with a low chance level of performance. Conditions in the three experiments reported here were used to maximize performance and therefore the SO motion results may be inflated to some degree. Thirdly, Dosher et al. used more complex displays that required the integration of multiple velocity signals over space and time. The simpler motion signals used here involved constant velocity signals at each point in time. Prazdny (1986) demonstrated that simple 3-D structure could be recovered from 2-D motion stimuli. This suggests that the recovery of 3-D structure from 2-D motion stimuli will occur if the stimulus is sufficiently simple and the task requirements are not too difficult. It appears that the image flow from translatory self-motion represents an elementary SO stimulus from which 3-D structure can be recovered.

As reported in previous vection research (Anderson and Braunstein, 1985) perceived depth appears to be an important factor in the vection experience. Anderson and Braunstein proposed that the ability level of radially expanding patterns to induce vection in central vision is determined by the effectiveness of the pattern in representing 3-D structure. They were able to demonstrate a similarity between depth ratings and vection induction of vection in response to an identical radial stimulus. MAE is perceived as object motion rather than self-motion and therefore internal depth may not be very important in MAE induction. A 2-D or 3-D object can equally be perceived as moving in space. The same cannot be said about self-motion which may explain why internal depth cues appear to have been more important in vection inducement than in MAE inducement. The radial carriers

consistently provided the longest vection durations. The noise and concentric carriers contained sufficient depth cues in the display to simulate 3-D structure from a 2-D image as evidenced by the fact that these carriers could induce moderate vection effects. However, under conditions of transparency, these carriers contained information which was inconsistent with image flow contained in natural self-motion vision patterns while the radial carrier did not contain such information. Subjective accounts that vection was not perceived in response to images with stationary backgrounds is consistent with the results of Heckman and Howard (1991). They found that when their subjects were presented with images at different depth planes, vection occurred when the image perceived to be at the farther depth plane was moving but not when the farther depth plane was perceived as a static image. When the farther depth plane was seen as a static image the display was perceived to represent object motion rather than self-motion.

Based on the absolute onset latencies and durations of the MAE and vection illusions, one might conclude that the FO versus SO distinction had a stronger effect in the case of MAE than in the case of vection. However, the direct comparison between absolute MAE and vection magnitude based on the results obtained in these experiments may be misleading for two reasons. Firstly, the stimuli were created in such a way as serve the dual purpose of eliciting the two illusions. That is, the vection stimuli served as the adapting stimuli for the MAE. Although the stimuli could effectively elicit the two illusions, no attempt was made to determine whether the stimuli drove the two illusions equally. From an empirical perspective, it would appear not to be the case. For example, vection strength is correlated with the size of the vection stimulus (Telford & Frost, 1993) while at small eccentricities MAE strength is weakened with increasing display sizes (Murakami & Shimojo, 1995). In view of the fact that large screen stimuli were used in all experiments, the magnitude of the MAE may have been relatively reduced. In an effort to equate the stimuli, one could use distance above threshold of the stimulus to detect the illusion as the measure by which to equate the stimuli but there is no evidence that the

vection and MAE illusions scale comparably in terms of this measure. Secondly, duration calculations included only the first MAE episode but multiple vection episodes. If only the first vection episode was counted in the calculation, the illusion strengths may have been more comparable for the two illusions.

While the response profiles for FO and SO stimuli were similar across the three different carrier patterns, the absolute magnitudes of the two illusions were highly affected by the choice of carrier pattern. In agreement with the results of the Smith et al. (1984) study, the presence of stationary texture in the background tended to suppress the magnitude of the MAE and vection effects perceived relative to the control stimulus. The only consistent exception to this effect occurred for the radial stimuli with explicit Fourier components, which elicited an effect equal or greater in magnitude to that of the control stimulus. The reasons why different carriers may affect the MAE and vection magnitudes differentially may be due to components within the combination of the combined carrier and modulator which contradict the motion signal. The dampening of the motion signal by the visual system in aggregation with the signals contradicting self-motion of the vestibular, tactile, and kinesthetic systems may provide enough information to overcome the effects of the illusions.

Physical plausibility may be important for both the MAE and vection illusions. MAEs for horizontal adapting directions are shorter (Mather, 1980). The patterns of visual flow normally experienced as the observer moves through the world (motion parallax) may serve to suppress detectors tuned to horizontal directions more than others. Since the stimuli used to evoke MAE in this study were radial, only a small portion of the image represented horizontal motion. Consequently, the signals representing other directions of motion in the display may have contributed more to the MAE percept. Vection was highly affected by the physical plausibility of the stimulus as evidenced by the subjects' reports of the absence of vection in response to component motion. In this case, component motion would be consistent with object motion rather than self-motion. Some subjects reported

that at higher check sizes of the noise stimulus, the checks appeared to be a screen through which they could see the moving modulator in the background. Under these circumstances, the magnitude of the vection experience was quite robust. Out of the three possible interpretations to this stimulus (coherent motion, checks as background, checks as foreground), this interpretation is the most consistent with natural image flow that occurs during self-motion. According to the composition of the stimuli, the checks should be seen as the background. However, this interpretation is inconsistent with the vection experience.

In conclusion, it is evident that SO motions can contribute to a process which supports motion in depth because SO motions were able to support the vection illusion under conditions where FO were minimized. SO motions were unable to support the MAE induced by radial images with static carriers. Therefore, the FO versus SO dichotomy was sufficient to explain MAE effects. MAE strength was positively related to the motion energy in the stimulus which makes the MAE a good indicator of the amount of motion energy in a visual display. Vection, on the other hand, was a poor indicator of the presence of motion energy and hence the vection results of Experiment 3 are difficult to explain entirely based on the FO versus SO distinction.

References

Adelson, E. H., & Bergen, J. R. (1985). Spatiotemporal energy models for the perception of motion. Journal of the Optical Society of America, 2, 284-299.

Adelson, E. H., & Movshon, J. A. (1982). Phenomenal coherence of moving visual patterns. Nature, 300, 523-525.

Albright, T. D. (1992). Form-cue invariant motion processing in primate visual cortex, Science, 261, 1141-1143.

Anderson, G. J. (1986). Perception of self-motion: Psychophysical and computational approaches. Psychological Bulletin, 99, 52-65.

Anderson, G. J., & Braunstein, M. L. (1985). Induced self-motion in central vision. Journal of Experimental Psychology: Human Perception and Performance, 11, 122-132.

Anderson, G. J., & Dyre (1989). Spatial orientation from optic flow in the central visual field. Perception and Psychophysics, 45, 453-458.

Baker, C. L., & Braddick, O. J. (1985). Eccentricity-dependent scaling of the limits for short-range apparent motion perception. Vision Research, 25, 803-812.

Badcock, D. R. and Derrington, A. M. (1989). Detecting the displacements of spatial beats: No role for distortion products. Vision Research, 29, 731-739.

Benton, C. P., & Johnston, A. (1977). First-order motion from contrast modulated noise? Vision Research, 37, 3073-3078.

Braddick, O. (1974). A short-range process in apparent motion. Vision Research, 14, 519-527.

Brandt, T., Dichgans, J., & Koenig, E. (1973). Differential effects of central versus peripheral vision on egocentric and exocentric motion perception. Experimental Brain Research, 16, 476-491.

Brandt, T., Wist, E. R., & Dichgans, J. (1978). Foreground and background in dynamic spatial orientation. Perception and Psychophysics, 17, 497-503.

Brown, R. O. (1995). Luminance nonlinearities and second-order stimuli. Poster presented at the Association for Research in Vision and Ophthalmology conference, Fort Lauderdale, FL.

Cavanagh, P. (1992). Attention-based motion perception. Science, 257, 1563-1565.

Cavanagh, P. & Mather, G. (1989). Motion: the long and short of it. Spatial Vision, 4, 103-129.

Chang, J. J., & Julesz, B. (1983). Displacement limits for spatial frequency filtered random-dot cinematograms in apparent motion. Vision Research, 23, 1379-1385.

Chubb, C. & Sperling, G. (1988). Drift-balanced random stimuli: A general basis for studying non-Fourier motion perception. Journal of the Optical Society of America, A, 5, 1986-2006.

Cropper, S. J. & Derrington, A. M. (1994). Motion of chromatic stimuli: first-order or second-order? Vision Research, 34, 49-58.

DeYoe, E. A. & Van Essen, D. C. (1985). Segregation of efferent connections and receptive field properties in visual area V2 of the macaque. Nature, 317, 58-61.

Derrington A. M. & Badcock, D. R. (1985). Separate detectors for simple and complex grating patterns? Vision Research, 25, 1869-1878.

Derrington A. M., Badcock, D. R. & Henning, G. B. (1993). Discriminating the direction of second-order motion at short stimulus durations. Vision Research, 33, 1785-1794.

Derrington A. M., Badcock, D. R. & Holroyd, S A.. (1992). Analysis of the motion of 2-dimensional patterns: Evidence for a second-order process. Vision Research, 32, 699-707.

Dosher, B. A., Landy, M. S., & Sperling, G. (1989). Kinetic depth effect and optic flow-I: 3D shape from Fourier motion. Vision Research, 29, 1789-1813.

Duffy, C. J., & Wurtz, R. H. (1991a). Sensitivity of MST neurons to optic flow stimuli. I. A continuum of response selectivity to large-field stimuli. Journal of Neurophysiology, 65, 1329-1345.

Duffy, C. J., & Wurtz, R. H. (1991b). Sensitivity of MST neurons to optic flow stimuli. II. Mechanisms of response selectivity revealed by small-field stimuli. Journal of Neurophysiology, 65, 1346-1359.

Gregory, R. L. (1985). Movement nulling: for heterochromatic photometry and isolating channels for 'real' and 'apparent' motion. Perception, 14, 193-196.

Gregory, R. L., & Harris, J. P. (1984). Real and apparent movement nulled. Nature, 307, 729-730.

Grzywacz, N. M. (1992). One-path model for contrast-independent perception of Fourier and non-Fourier motions. Investigative Ophthalmology & Visual Science, 33, 954.

Gurnsey, R., Fleet, D. & Potechin, C. (1998). Second-order motions contribute to vection. Vision Research, 38, 2801-2816.

Harris, L. R., & Smith, A. T. (1992). Motion defined exclusively by second-order characteristics does not evoke optokinetic nystagmus. Visual Neuroscience, 9, 565-570.

Heckman, T. & Howard, I. P. (1991). Induced motion: isolation and dissociation of egocentric and vection-entrained components. Perception, 20, 285-305.

Howard, I. P. & Heckman, T. (1989). Circular vection as a function of the relative sizes, distances, and positions of two competing visual displays, Perception, 18, 657-665.

Johansson, G. (1977). Studies on visual perception of locomotion. Perception, 6, 365-376.

Landy, M. S., Dosher, B. A., Sperling, G., & Perkins, M. E. (1991). The kinetic depth effect and optic flow-II: first- and second-order motion. Vision Research, 31, 859-876.

Ledgeway, T. & Smith, A. (1994). Evidence for separate motion-detecting mechanisms for first- and second-order motion in human vision. Vision Research, 34, 2727-2740.

Lishman, J. R., & Lee, D. N. (1973). The autonomy of visual kinaesthesis. Perception, 2, 287-294.

Livingstone, M. and Hubel, D. (1988). Segregation of form, color, movement, and depth: Anatomy, physiology, and perception. Science, 240, 740-749.

Mather, G. (1980). The movement aftereffect and a distribution-shift model for coding the direction of visual movement. Perception, 9, 379-392.

Mather, G., and West., S. (1993). Evidence for second-order motion detectors. Vision Research, 33, 1109-1112.

McCarthy, J. E. (1993). Directional adaptation effects with contrast modulated stimuli. Vision Research, 33, 2653-2662.

Merigan, W. H., and Maunsell, J. H. R. (1993). How parallel are the primate visual pathways? Annual Review of Neuroscience, 16, 369-402.

Murakami, I. & Shimojo, S. (1995). Modulation of motion aftereffect by surround motion and its dependence on stimulus size and eccentricity. Vision Research, 35, 1835-1844.

Nakayama, K. (1985). Biological image motion processing: A review. Vision Research, 25, 625-660.

Nishida, S., Ashida, H. & Sato, T. (1994). Complete interocular transfer of motion aftereffect with flickering test. Vision Research, 34, 2707-2716.

Nishida, S., Ledgeway, T., & Edwards, M. (1997). Dual multiple-scale processing for motion in the human visual system. Vision Research, 37, 2685-2698.

Nishida, S., & Sato, T. (1995). Motion aftereffect with flickering test patterns reveals higher stages of motion processing. Vision Research, 35, 477-490.

Nishida, S., & Sato, T. (1993). Two kinds of motion aftereffect reveal different types of motion processing. Investigative ophthalmology & visual science, 34, 1363.

Ohmi, M., Howard, I. P., & Landolt, J. P. (1987). Circular vection as a function of foreground-background relationships. Perception, 16, 17-22.

Perrone, J. A., & Stone, L. S. (1994). A Model of self-motion estimation within primate extrastriate visual cortex. Vision Research, 34, 2917-2938.

Post, R. B. (1988). Circular vection and stimulus eccentricity. Perception, 17, 737-744.

Potechin, C. (1995). The influence of stimulus motion order and perceived reality of the stimulus on the inducement of vection. Unpublished Honors thesis, Concordia University.

Prazdny, K. (1986). Three-dimensional structure from long-range apparent motion. Perception, 15, 619-625.

Reichardt, W. (1961). Autocorrelation, a principle for the evaluation of sensory information by the central nervous system. In W. A. Rosenblith (Ed.), Sensory communication (pp. 303-317) New York: Wiley.

Sauvan, X. M., & Bonnet, C. (1993). Properties of curvilinear vection. Perception and Psychophysics, 53, 429-435.

Savoy, R. L. (1987). Contingent aftereffects isoluminance: Psychophysical evidence for separation of color, orientation and motion. Computer Vision, Graphics, and Image Processing, 37, 3-19.

Smith, A. T. (1994). Correspondence-based and energy-based detection of second-order motion in human vision. Journal of the Optic Society of America A., 11, 1294-1948.

Smith, A. T., Hess, R. F., & Baker Jr., C. L. (1994). Direction identification thresholds for second-order motion in central and peripheral vision. Journal of the Optic Society of America A., 11, 506-514.

Smith, A. T. & Ledgeway, T. (1997). Separate detection of moving luminance and contrast modulations: fact or artifact? Vision Research, 37, 45-62.

Smith, A. T., Musselwhite, M. J., & Hammond, P. (1984). The influence of background motion on the motion aftereffect. Vision Research, 24, 1075-1082.

Stoner, G. R., & Albright, T. D. (1992). Neural correlates of perceptual motion coherence. Nature, 358, 412-414.

Stoner, G. R., Albright, T. D., Ramachandran, V. S. (1990). Transparency and coherence in motion perception. Nature, 344, 153-155.

Telford, L & Frost, B. J. (1993). Factors affecting the onset and magnitude of linear vection. Perception and Psychophysics, 53, 682-692.

Telford, L., Spratley, J., & Frost, B. J. (1992). Linear vection in the central visual field facilitated by kinetic depth cues. Perception, 21, 337-349.

Turano, K. (1991). Evidence for a common motion mechanism of luminance-modulated and contrast-modulated patterns: selective adaptation. Perception, 20, 455-466.

Turano, K. & Pantle, A. (1989). On the mechanism that encodes the movement of contrast variations: velocity discrimination. Vision Research, 29, 207-221.

Ullman, S. (1979). The interpretation of visual motion. Mass: The MIT Press.

Van Santen, J. P. H. and Sperling, G. (1985). Elaborated Reichardt detectors. Journal of the Optic Society of America A., 2, 300-321.

Verstraten, F. A. J., Fredericksen, R. E., Van Wezel, R. J. A., Lankheet, M. J. M., & Van de Grind,W. A. (1995). Recovery from adaptation for dynamic and static motion aftereffects: Evidence for two mechanisms. Vision Research, 36, 421-424.

Von Grünau, M. (1996). A motion aftereffect for long-range apparent motion. Perception and Psychophysics, 40, 31-38.

Von Grünau, M., & Dubé, S. (1993). Ambiguous plaids: Switching between coherence and transparency. Spatial Vision, 3, 199-211.

Wade, N. J. (1994). A selective history of the study of visual motion aftereffects. Perception, 23, 1111-1134.

Watson , A. B., & Ahumada, A. J. (1985). Model of human visual-motion sensing. Journal of the Optic Society of America A., 2, 322-341.

Wilson, H. R., Ferrera, V. P., and Yo, C. (1992). A psychophysically motivated model for two-dimensional motion perception. Neuroscience, 9, 79-97.

Zanker, J. (1994a). Modeling Human Motion Perception. I. Classical stimuli. Naturwissenschaften, 81, 156-163.

Zanker, J. (1994b). Modeling Human Motion Perception. II. Beyond Fourier motion stimuli. Naturwissenschaften, 81, 200-209.

Zanker, J. M. (1993). Theta motion: A paradoxical stimulus to explore higher order motion extraction. Vision Research, 33, 553-569.

Zhou, Y. X., & Baker Jr., C. L. (1993). A processing stream in mammalian visual cortex neurons for non-Fourier responses. Science, 261, 98-100.

Appendix A

Descriptive statistics for latency to onset for experiments 1, 2, and 3

Table A1

Descriptive statistics for latency to onset: experiment 1

Experiment 1		First Order	Second Order
Motion aftereffect			
Concentric			
	M	1.53	7.01
	SD	0.93	4.03
Radial			
	M	1.20	0.84
	SD	0.65	0.14
Noise			
	M	0.87	9.54
	SD	0.17	4.83
Control			
	M	1.16	
	SD	0.57	
Vection			
Concentric			
	M	16.40	18.91
	SD	9.61	9.89
Radial			
	M	5.97	8.77
	SD	5.74	6.39
Noise			
	M	17.98	21.70
	SD	12.33	9.83
Control			
	M	5.32	
	SD	5.78	

Table A2

Descriptive statistics for latency to onset: experiment 2

Experiment 2		First Order n = -1	First Order n = 1	Second Order n = 0
Motion aftereffect				
Concentric				
	M	2.39	3.07	5.52
	SD	2.24	5.17	7.04
Radial				
	M	1.75	2.14	3.62
	SD	2.40	3.28	6.12
Noise				
	M	2.12	2.88	9.74
	SD	3.23	5.11	9.64
Control				
	M		3.92	
	SD		7.57	
Vection				
Concentric				
	M	6.83	5.07	9.85
	SD	5.94	4.31	9.51
Radial				
	M	2.95	3.57	5.41
	SD	2.58	3.54	4.83
Noise				
	M	9.36	8.69	13.00
	SD	7.55	8.54	11.42
Control				
	M		2.90	
	SD		1.88	

Table A3

Descriptive statistics for latency to onset: experiment 3

Experiment 3		Motion aftereffect	Vection
Noise unit size (in pixels)			
1			
	M	5.52	5.06
	SD	7.12	3.89
2			
	M	5.14	6.71
	SD	6.53	5.29
4			
	M	3.07	5.87
	SD	3.93	4.44
8			
	M	1.90	6.52
	SD	1.61	6.04
16			
	M	1.55	4.58
	SD	1.61	3.67
32			
	M	1.58	4.52
	SD	1.73	4.69
64			
	M	2.35	3.50
	SD	2.58	2.30
128			
	M	2.63	3.32
	SD	2.45	2.28
Control			
	M	3.47	2.67
	SD	3.78	2.26

Appendix B

Descriptive statistics for duration for experiments 1, 2, and 3

Table B1

Descriptive statistics for duration: experiment 1

Experiment 1		First Order	Second Order
Motion aftereffect			
Concentric			
	M	6.02	1.22
	SD	2.06	0.97
Radial			
	M	9.64	6.18
	SD	2.80	3.31
Noise			
	M	5.86	0.75
	SD	2.01	1.33
Control			
	M	8.14	
	SD	1.68	
Vection			
Concentric			
	M	8.35	5.78
	SD	8.66	7.94
Radial			
	M	20.14	15.38
	SD	8.50	8.53
Noise			
	M	8.24	5.05
	SD	11.98	7.80
Control			
	M	19.55	
	SD	8.96	

Table B2

Descriptive statistics for duration: experiment 2

Experiment 2		First Order n = -1	First Order n = 1	Second Order n = 0
Motion aftereffect				
Concentric				
	M	5.50	3.88	1.73
	SD	3.54	2.32	1.69
Radial				
	M	10.93	8.58	4.88
	SD	3.83	2.39	1.78
Noise				
	M	6.42	5.02	0.96
	SD	2.52	2.71	1.36
Control				
	M		6.29	
	SD		4.70	
Vection				
Concentric				
	M	17.57	18.89	12.44
	SD	8.44	7.21	8.94
Radial				
	M	24.90	25.15	22.57
	SD	4.05	5.09	6.94
Noise				
	M	17.76	16.44	11.27
	SD	11.05	10.51	9.69
Control				
	M		26.33	
	SD		2.74	

Table B3

Descriptive statistics for duration: experiment 3

Experiment 3		Motion aftereffect	Vection
Noise unit size (in pixels)			
1			
	M	1.28	11.72
	SD	1.03	3.43
2			
	M	1.15	9.76
	SD	1.18	3.13
4			
	M	3.82	10.49
	SD	2.89	2.62
8			
	M	6.23	10.13
	SD	3.83	4.07
16			
	M	7.24	11.29
	SD	4.72	1.45
32			
	M	7.40	12.98
	SD	4.75	3.30
64			
	M	8.66	12.54
	SD	4.21	2.88
128			
	M	8.07	13.69
	SD	4.70	2.52
Control			
	M	7.40	17.28
	SD	6.32	2.52

Appendix C

Subjective isoluminance points for the subjects in experiments 1 & 2

Table C1

Subjective isoluminance points for the subjects in experiment 1

Subject Number	*n* values		
	Concentric	Radial	Noise
1	-0.050	-0.050	-0.050
2	0.000	0.000	0.000
3	0.000	0.025	-0.025
4	0.000	0.000	0.000
5	0.050	0.000	-0.050

Table C2

Subjective isoluminance points for the subjects in experiment 2

Subject Number	*n* values		
	Concentric	Radial	Noise
1	0.00	-0.05	-0.05
2	0.00	0.00	0.00
3	0.00	-0.05	0.00
4	0.00	0.00	0.00
5	0.00	0.05	0.00